The Transition Between the Complex Quadratic Map and the Hénon Map

by

Sarah N. Kabes

Technical Report

Department of Mathematics and Statistics
University of Minnesota
Duluth, MN 55812

July 2012

The Transition Between the Complex Quadratic Map and the Hénon map

A PROJECT SUBMITTED TO THE FACULTY OF THE GRADUATE SCHOOL OF THE UNIVERSITY OF MINNESOTA
BY

Sarah Kabes

in partial fulfillment of the requirements
for the degree of Master of Science

July 2012

Acknowledgements

Thank you first and foremost to my advisor Dr. Bruce Peckham. Your patience, encouragement, excitement, and support while teaching have made this experience not only possible but enjoyable as well. Additional thanks to my committee members, Dr. Marshall Hampton and Dr. John Pastor for reading and providing suggestions for this project.

Furthermore, without the additional assistance from two individuals my project would not be as complete as it is today. Thank you Dr. Harlan Stech for finding the critical value $h = \frac{5}{12}$, and thank you Scot Halverson for working with me and the open source code to produce the movie.

Of course none of this would be possibly without the continued support of my family and friends. Thank you all for believing in me.

Abstract

This paper investigates the transition between two well known dynamical systems in the plane, the complex quadratic map and the Hénon map. Using bifurcation theory, an analysis of the dynamical changes the family of maps undergoes as we follow a "homotopy" from one map to the other is presented. Along with locating common local bifurcations, an additional un-familiar bifurcation at infinity is discussed. Results and images are given for many, but not all possible parameter values with the help of *Mathematica v.*7. Conclusions drawn provide insight into bifurcation phenomena for dynamical systems and suggest new and/or additional research opportunites.

TABLE OF CONTENTS

Abstract

This paper investigates the transition between two well known dynamical systems in the plane, the complex quadratic map and the Hénon map. Using bifurcation theory, an analysis of the dynamical changes the family of maps undergoes as we follow a "homotopy" from one map to the other is presented. Along with locating common local bifurcations, an additional un-familiar bifurcation at infinity is discussed. Results and images are given for many, but not all possible parameter values with the help of *Mathematica v.*7. Conclusions drawn provide insight into bifurcation phenomena for dynamical systems and suggest new and/or additional research opportunites.

1.Introduction

According to Hirsch, Smale, and Devaney, in the textbook *Differential Equations, Dynamical Systems & An Introduction to Chaos:* "A *dynamical system* is a way of describing the passage in time of all points of a given space $\boldsymbol{S}$." Given a function $f: X \to X$, where the given space here is X, with an initial condition $x_0 \in X$ we define orbits by $x_{n+1} = f(x_n)$. This collection of orbits is a discrete dynamical system, and the type of dynamical systems in this paper. Importantly, Hirsch, Smale, and Devaney explain that dynamical systems techniques are used when, "higher dimensional systems may exhibit chaotic behavior, a property that makes knowing a particular explicit solution essentially worthless in the larger scheme of understanding the behavior of the system."

Moreover, in a second book by Devaney, titled, *An Introduction to Chaotic Dyanmical Systems*, he discusses bifurcation theory in section 1.12. Defining bifurcation as "a division in two, a splitting apart, a change." He mentions that, "the object of bifurcation theory is to study the changes that maps undergo as parameters change. These

changes often involve the periodic point structure, but may also involve other changes as well."

Using dynamical system theory, including bifurcation theory, and analyzing graphical evidence, this project looks at the dynamics of a family of maps that is a homotopy from the complex quadratic map, Q_c, to the Hénon map, H. Since Q_c is a map of $\mathbb{C}^1$ and H is a map of $\mathbb{R}^2$, it was necessary to apply a conjugacy between $\mathbb{C}^1$ and $\mathbb{R}^2$, so that all maps were on the same space, $\mathbb{R}^2$. This form was also easier to code and analyze with the software. When applied to a pair of maps, a homotopy generates a new family of maps that is a connection between the two previous maps; the idea behind this method being to provide the investigator with a connection between the two maps, or new information about similar maps.

The homotopy implemented for this project is of the general, "straight line" form: $h * f(x,y) + (1-h) * g(x,y)$. Here $f(x,y)$ represents one map from $\mathbb{R}^2 \to \mathbb{R}^2$, $g(x,y)$ another, different map from $\mathbb{R}^2 \to \mathbb{R}^2$, and h the homotopic parameter that changes the map. As h varies on the interval $[0,1]$ our maps change from $g(x,y)$ to $f(x,y)$ and provide us with a one-parameter family of maps.

In the following sections this paper looks sequentially (in h) at the homotopy and the dynamics and bifurcations of its maps. The study begins with bounded and unbounded orbits, computed by establishing escape radii. Snap shots of attractors and their identification are addressed next. An orbit diagram is then presented, as a look at attracting behavior with much smaller increments in h. After these first four sections, the paper continues with period one and period two points, and their locations, critical sets, J_0, and bifurcation classification including stability analysis. Concluding the prior sections are conglomerate snap shots of representative h-values used to analyze the homotopy and an assessment of the transition between Q_c and H as a whole.

2.Definition of the Homotopic Family of Maps

This paper begins with a summary of two well known maps: the complex quadratic map's filled Julia set (when $c = -1$) and the Hénon map, as well as an understanding of the conjugacy conversions and formation of the homotopy. Once formulated, this paper's goal is to investigate the bifurcations of the family of maps produced from the homotopy as h varies on $[0,1]$.

2.1.The Quadratic Map

The Douady-Hubbard family of quadratic polynomials or simply the quadratic family, $Q_c(z) = z^2 + c$, is one of the most recognized complex dynamics families. More specifically, the quadratic map, $Q_{-1}(z) = z^2 - 1$, referred to in this paper as the basilica map, is a fairly common map to study for its chaotic behavior. Since this representation is a mapping from $\mathbb{C}^1 \to \mathbb{C}^1$ and because its opposite end counterpart, the Hénon map, is a discrete-time dynamical system from $\mathbb{R}^2 \to \mathbb{R}^2$, it makes sense to convert the basilica map into a real map so as to keep the homotopy in consistent planes. Conversion was completed with the use of a conjugacy as such:

Define the conjugacy:

$$f(x,y) = h\left(Q_c\left(h^{-1}(x,y)\right)\right)$$

where $h: \mathbb{C}^1 \to \mathbb{R}^2$ is defined by $h(x+iy) = (x,y)$.

(Recall the definition of a complex number, $z = x + iy$.)

Apply h^{-1} with the definition:

$$f(x,y) = h\left(Q_{-1}\left(h^{-1}(x+iy)\right)\right)$$

Apply Q_{-1}:

$$f(x,y) = h\big(Q_{-1}((x+iy)^2 + (-1+i*0))\big)$$

Expand and collect terms:

$$f(x,y) = h\big(x^2 - y^2 - 1 + i(2xy+0)\big)$$

Then apply h:

$$f(x,y) = (x^2 - y^2 - 1, 2xy)$$

Therefore the final conversion is:

$$Q_{-1}(z) = z^2 - 1 \Leftrightarrow f(x,y) = (x^2 - y^2 - 1, 2xy)$$

This final form is the one used throughout the paper:

$$f(x,y) = (x^2 - y^2 - 1, 2xy)\,. \qquad (1)$$

2.2.The Hénon Map

As stated previously, the Hénon map is a discrete-time dynamical system, as is the quadratic map, but it is set in the real plane. Originally established as a simplified model of the Poincaré section of the Lorenz model, the Hénon map, $H(x,y) = (1 - ax^2 + y, bx)$, is one of the simplest settings for complex behavior. Analyses included in this paper make particular use of the canonical Hénon map, which implements the parameter values: $a = 1.4$ and $b = 0.3$, yielding:

$$H(x,y) = (1 - 1.4x^2 + y, 0.3x)\,. \qquad (2)$$

This version of the Hénon map displays chaotic behavior on a "strange attractor."

2.3.The Homotopy's Full Form

With the maps as stated above, the homotopy studied in this paper is:

$$g_h(x,y) = h * H(x,y) + (1-h) * f(x,y). \quad (3)$$

The reason for this homotopy is to study bifurcations in the transition from the basilica map to the Hénon map. The organization of the paper takes place as follows:

- Bounded vs unbounded orbits and escape radii
- Attractors
- Periodic points
- Critical sets
- Bifurcation Classification
- Summary

3.Bounded vs. Unbounded Orbits and Escape Radii

Identifying points whose orbits remain bounded and points whose orbits go off to infinity (are unbounded) helps understand the dynamics of a map. Notations for these regions are as follows:

$$K_h = \{(x,y): g_h(x,y) \nrightarrow \infty\}$$

$$J_h = \partial K_h$$

$$B_h = K_h \backslash J_h = K_h^{\circ}$$

That is, K_h is the subset of bounded points, J_h is the boundary of K_h, and B_h is the interior of K_h.

Note: These names are common notation for complex maps, more specifically the quadratic map, but are being implemented here to the

family of maps and so they do not have all the same properties as they would for the quadratic map.

Often times in complex dynamics orbits starting in B_h approach an attractor after subsequent iteration. For that reason, it was logical and critical to this project to begin with the identification of these sets for the homotopy as h varied on the interval $[0,1]$. Step one was whether or not they could be produced for the entire family of maps. If producing these were not possible, then the numerical computation of them could not proceed, and as such further investigation for these maps would be difficult. Computation of these orbits in *Mathematica* required an "escape algorithm" for each h. The escape algorithm used was:

1. Determine an escape radius (as described below)
2. For each point within a defined grid, apply the map. Test to see whether the distance that point is from the origin is beyond the escape radius. Repeat if not.
3. Record the number of iterations necessary to escape up to some maximum.

   Note: If a point has not escaped by the maximum number of iterates, we assume it remains bounded, but there does exist some bias here. If the number of iterates is increased we may in fact get a smaller bounded region, and as such, if the number of iterates is decreased we may have a larger bounded region than the actual/theoretical one.

4. Plot these values for each point.

   Note: Images later were created with a "DensityPlot" in *Mathematica* for a maximum of 150 "PlotPoints". This command creates an image with "n" (150) initial points in each coordinate direction.

In addition to the creation of the bounded and unbounded sets of orbits for fixed h-values within *Mathematica*, the manipulation of an open source code [3] generating a movie of the smooth transition of these sets as h varied, led to an important realization. While all bounded vs. unbounded sets could be approximated using the escape algorithm, no one escape radius gave a fully accurate image of every K_h. This insight led to an investigation of escape radii.

3.1.Nien's Lemma 2.2

An escape radius provides a disk that encloses the bounded orbits; it can also include some of the unbounded orbits, but more importantly guarantees that points outside it diverge to infinity. Making use of an article in the International Journal of Bifurcation and Chaos, Vol. 8, No. 1, entitled *The Dynamics of Planar Quadratic Maps with Nonempty Bounded Critical Set* by Chia-Hsing Nien, this escape radius, K, can be found for any planar quadratic map, $F(x,y)$:

$$F(x,y) = \big(f_1(x,y), f_2(x,y)\big) \text{ where}$$
$$f_1(x,y) = a_0x^2 + a_1xy + a_2y^2 + a_3x + a_4y + a,$$
$$f_2(x,y) = b_0x^2 + b_1xy + b_2y^2 + b_3x + b_4y + b$$

Nien's lemma states that, "If the origin is not in the image of the unit circle under the [polar] mapping G," where G is the quadratic terms of F,

$$G(x,y) = (a_0x^2 + a_1xy + a_2y^2, b_0x^2 + b_1xy + b_2y^2)$$

then there exists a positive real number K such that successive iterates end up twice as far from the origin. In his proof, Nien notes that "the assumption on the image of the unit circle under the mapping G, implies:

$$inf_{\theta\in[0,2\pi]}|G(\cos\theta, \sin\theta)| = \delta > 0\,."$$

That is, there exists a point on the image of the unit circle that is the smallest distance from the origin, δ. From the triangle inequality, and since $\delta > 0$, we can choose a $K > 0$ such that:

$$(K\delta - |a_3 \cos\theta + a_4 \sin\theta\,, b_3 \cos\theta + b_4 \sin\theta| - [|(a,b)|/K]) > 2, \forall\theta \in [0, 2\pi]\,. \quad (4)$$

After the unit circle was mapped, this delta was calculated for those fixed h values, using the quadratic terms of the homotopy, $g_h(x,y)$. That is, using the equation:

$$G_h(x,y) = (-1.4hx^2 + (1-h) * (x^2 - y^2), (1-h) * 2xy)\,. \quad (5)$$

These images showed for which values of h a positive escape radius existed. Figure 1 below displays the image of the unit circle under each mapping.

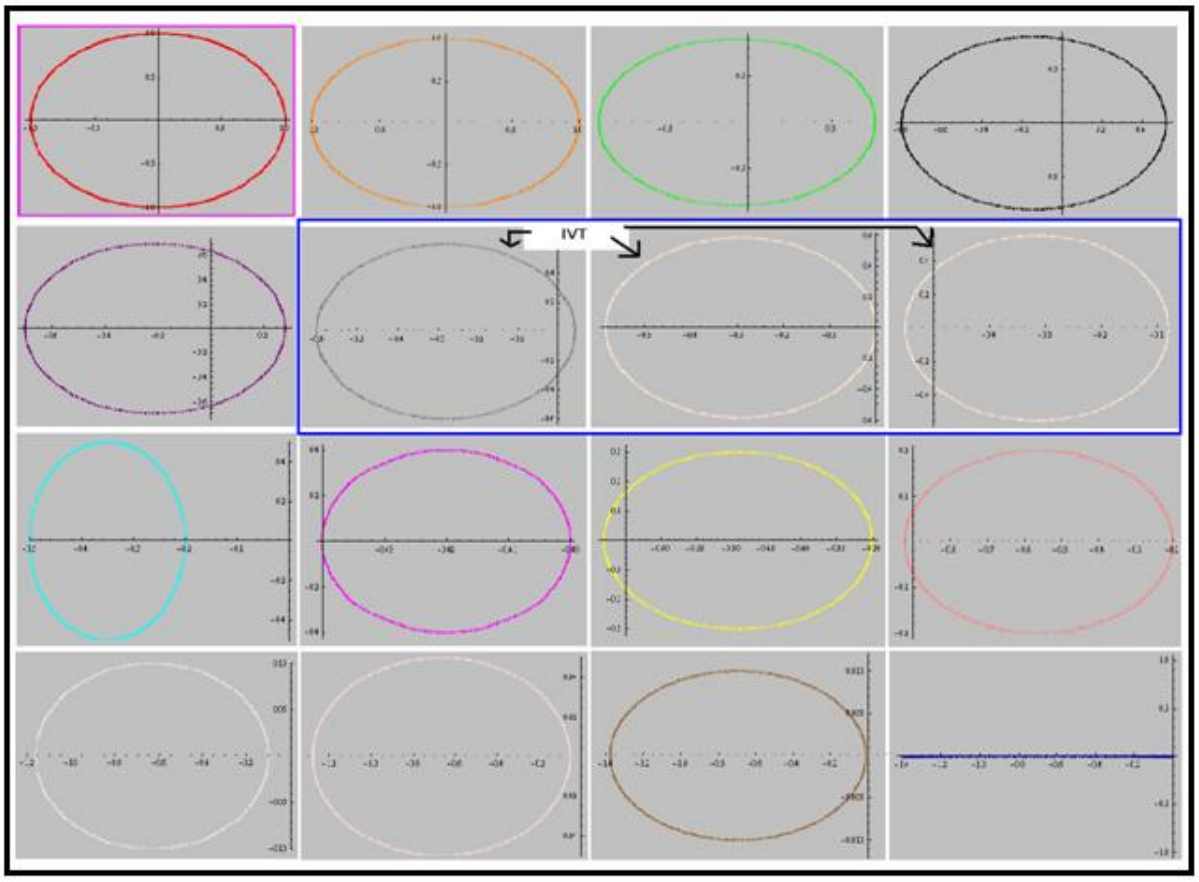

Figure 1 (caption on next page)

Mapped Unit Circle Progression

The first image is the un-mapped unit circle (for reference), the following images are for $h = 0, 0.1, 0.2, 0.3, 0.4, 0.417, 0.45, 0.5, 0.6, 0.7, 0.8, 0.9, 0.95, 0.99, 1$

Since a property of continuous functions is the intermediate value theorem (IVT), we know from the transition of the graphics above that there is a h value between 0.4 and 0.45 where the origin is in the image of the mapped unit circle. This indicates the corresponding K value is infinite, and so equation (4) was solved for K so this could be verified. Taking the positive root of the equation, with coefficients depending on h, Table 1 below gives the numerical values of each radius calculated and shows that as h approaches the critical value, which turns out to be $h = \frac{5}{12}$, successive escape radii get larger and larger. This event mirrors what occurs just before h reaches 1, the Hénon map.

h-value	K-value
0	3.0
0.1	3.1402633744693786
0.2	4.567590481430012
0.3	8.508122571817713
0.4	60.24896692450835
0.41	150.86941666717217
0.415	603.9921389130382
0.416666666666	DNE
0.418	755.8656181676062
0.42	302.73947983275934
0.45	30.84786791485802
0.5	12.696898479113813
0.6	6.6503676271838605
0.7	9.109772228646444
0.8	14.071067811865476
0.9	29.034441853748632
0.95	59.016944286290894
0.99	299.00334444419633
0.995	599.001669444429
1	DNE

Table 1

Escape radii for different h-values.

As seen above, both $h = \frac{5}{12}$ and $h = 1$ appear to be parameter values for which the escape radius, guaranteed my Nien's Lemma is infinite. In Figure 1, the mapped unit circle for $G_1(x, y)$ (the quadratic terms of the Hénon map) is shown to include the origin in the bottom right image. In order to verify what is shown, the two points found to map from the unit circle to the origin by equations (1), (2), and (3)are: $(0,1) \mapsto (0,0)$ and $(0,-1) \mapsto (0,0)$. Plugging in $h = \frac{5}{12}$, Figure 2 displays the mapped unit circle for $G_{\frac{5}{12}}(x, y)$. This value, too, was verified by finding the points that map from the unit circle to the origin. They are: $(1,0) \mapsto (0,0)$ and $(-1,0) \mapsto (0,0)$.

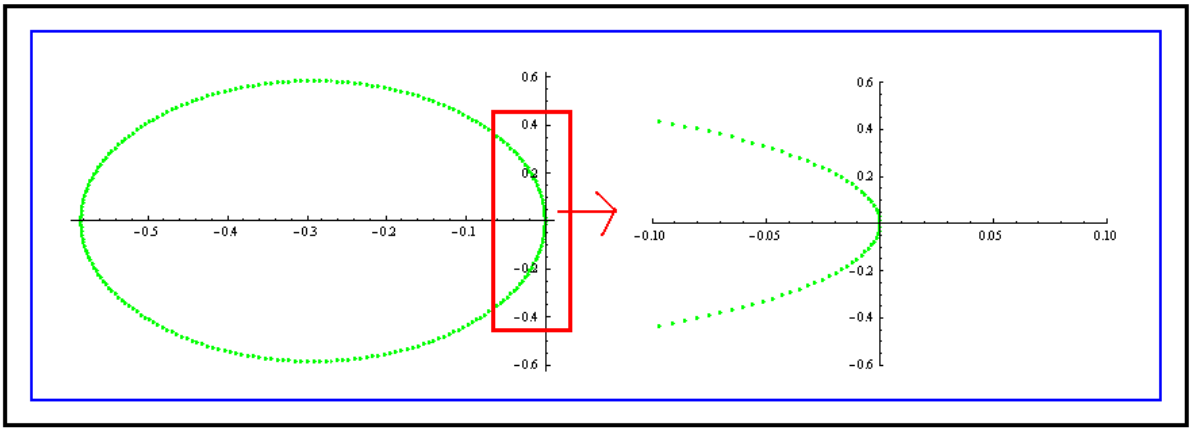

Figure 2

Mapped unit circle for $h = \frac{5}{12}$.

Note: For the basilica map, the escape radius most commonly used to produce graphical images of its basin is two. However the Nien equation led to an escape radius of three since it required distances from the origin to double. It is important to note that an escape radius of three still guarantees that any points outside of it diverge to infinity. Furthermore, points in B_0, the interior of the basilica map's bounded orbits, tend to a single period two attractor, while

points in the Julia set remain on the boundary. For the Hénon map a frequently chosen K to depict the basin is ten. However, there does not actually exist a positive real-valued K that is an escape radius for the Hénon map. This is because the Hénon map's basin boundary extends to infinity. Points in this unbounded basin, B_1 tend to a chaotic strange attractor. (For the images of the Hénon map within this paper the escape radius used was 900.)

3.2.Bounded Orbit Visualization

With the help of a lab assignment from the University of North Carolina at Asheville [5], initial development of the escape algorithm for the basilica map, and visualization of the bounded and unbounded orbits, took place in the complex plane. Once converted to the real plane via conjugacy, application of the escape algorithm produced Figure 3 below. The basilica map is so called because its filled Julia set resembles St. Peter's basilica. Uniquely, it contains numerous "bulbs" upon bulbs.

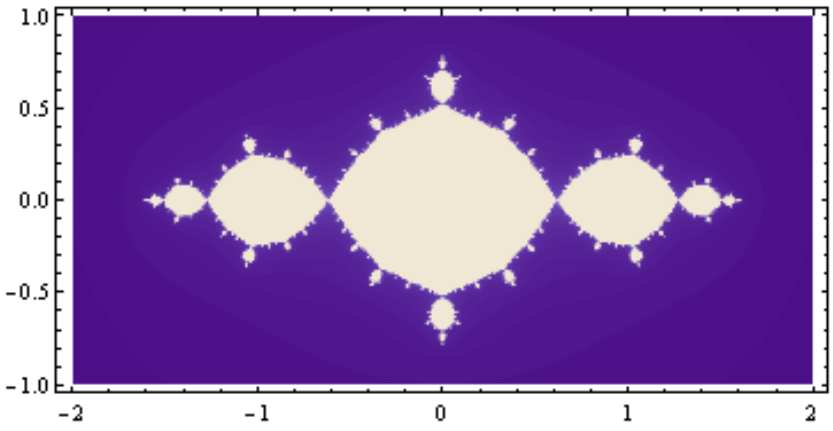

Figure 3

The basilica map's basin of attraction

(See text below for coloring scheme)

The Hénon map's basin of attraction is drastically different. In the shape of a stretched letter U, this basin extends to infinity. Figure 4 depicts the Hénon map's basin.

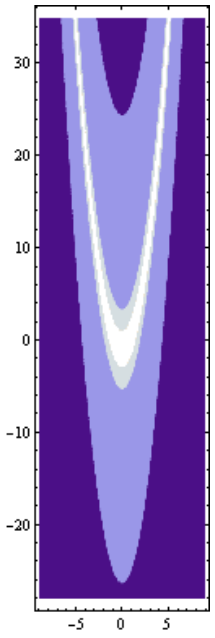

Figure 4

The Hénon map's basin of attraction.

Note: The different colors depicted in the basin images represented the different count values. That is, they represent points that remain bounded or alternatively how long points take to escape. The white/cream color illustrates points that remain bounded, the shades of blue/purple represent points that are unbounded and head off to infinity, with lighter shades taking a longer time to escape.

Quite interesting is how each set of initial conditions corresponding to bounded orbits change as the parameter, h changes. From a bulbous basilica map basin, to an unbounded U shaped Hénon basin, the intermediate bounded regions range from twisted and stretched versions of the basilica map to more simple diamonds and ovals, which then open and stretch as h approaches 1. Figure 5 on the following page illustrates the evolution of these regions with fifteen

snapshots. Each consecutive basin was produced by changing the h value by approximately one tenth. However, smaller h values were used near interesting periodic points like $h = \frac{5}{12}$ and $h = 1$. Notice that images 6 and 7 look very similar, but image 6's x-axis extends much farther than image 7's x-axis which is bounded between -20 and 20. This is because in between these two images, at $h = \frac{5}{12}$, the bounded orbit set, K_h, extends to infinity. Also notice that for images 12 and 13, $K_{.9}$ and $K_{.95}$ are connected sets, but not simply connected sets as the $K_h's$ appear to be for the other images.

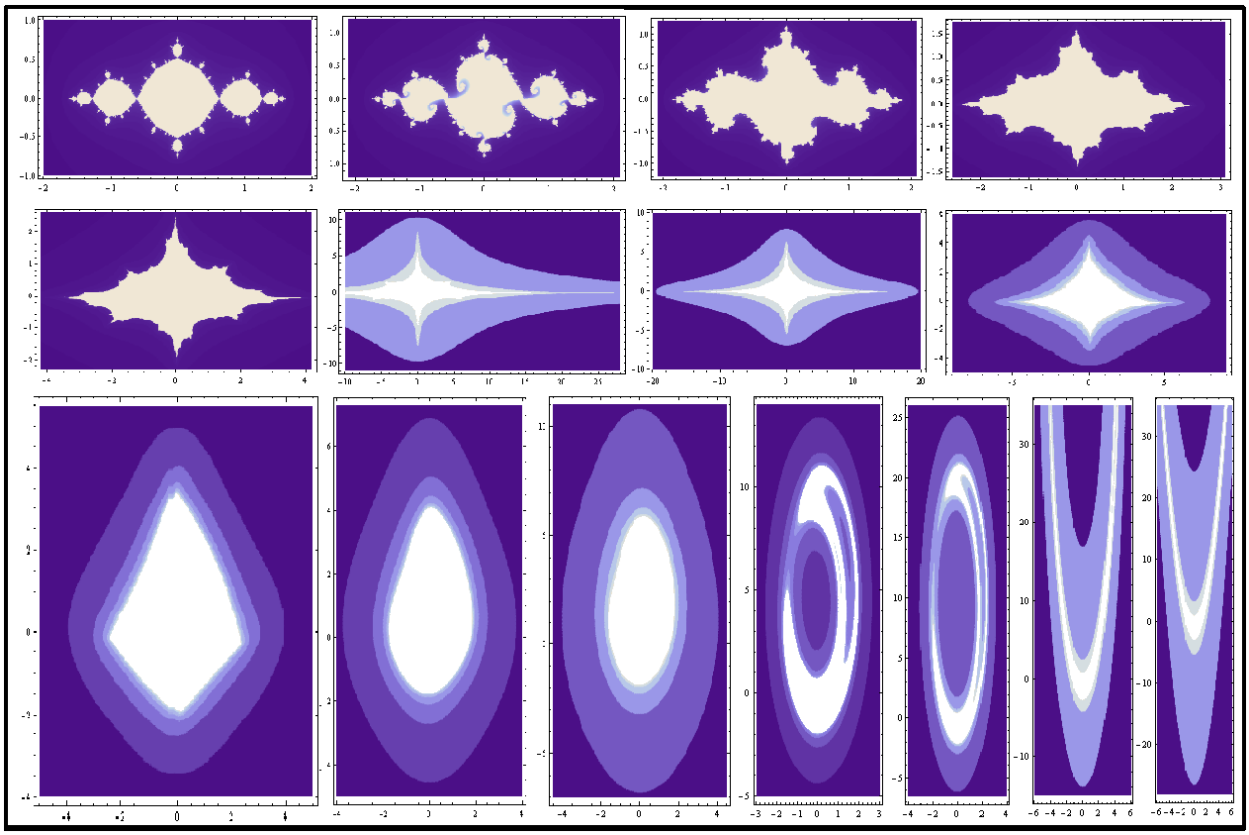

Figure 5

Evolution of the basins of attraction as h continues on $[0,1]$. The specific h-values here are: $h = 0, 0.056, 0.1, 0.2, 0.3, 0.4, 0.45, 0.5, 0.6, 0.7, 0.8, 0.9, 0.95, 0.99, 1$.

4.Attractors

While theoretically possible for this homotopy to possess maps with multiple attractors within the bounded set, B_h, numerical investigation has not shown any. For all maps involved in this homotopy, there appears to be but one attractor within any map's region of bounded orbits.

This was concluded with the support of the *TBC* software – a software created by Dr. Bruce Peckham specifically used for the graphical investigation of maps. Able to graph a fine grid of each map's bounded and unbounded orbits, *TBC* could then iterate all points within B_h at once. This iteration appeared to go to a single object for all fixed h-values tested. This numerically corroborates that for any individual point within the basin its resulting behavior is to end up at a single attractor – be it some periodic orbit, or a strange attractor. Therefore, B_h appears to be the basin of attraction for that map's attractor.

The basilica map and Hénon map are both well-studied. It is known that the basilica map has a period two attractor at the points $(-1,0)$ and $(0,0)$, and the Hénon map has a strange attractor that is crescent shaped and confined within the range: $-4 \leq x \leq 4$ and $-3 \leq y \leq 3$. Figure 6 following, illustrates these two wholly different attractors.

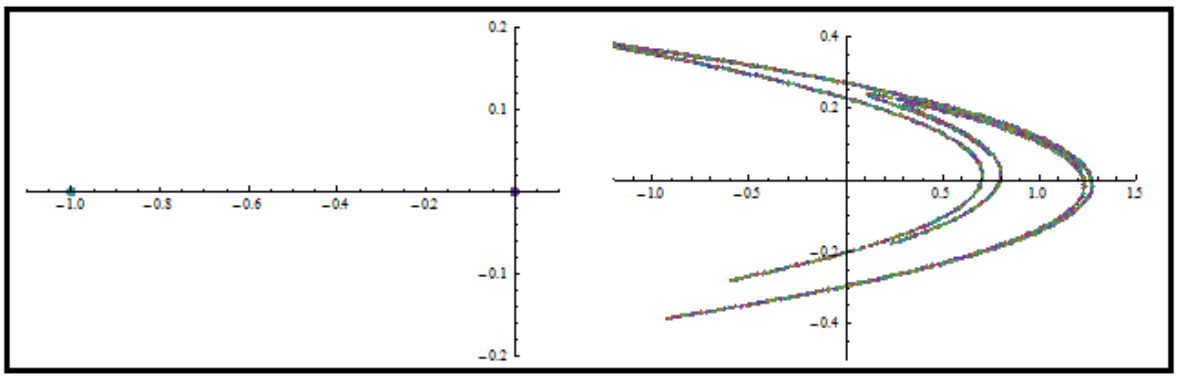

Figure 6

The basilica map and Hénon map attractors.

4.1.Attractor Identification

The above attractors, and likewise the following orbits and attractors, were identified using *Mathematica* in the same manner. The process was:

1. Beginning with the quadratic map and its known period two attractor, set $h = 0$ and iterate a fixed number of times from $(0,0)$.
2. For following fixed h-values, iterate from the ending point of the orbit for the previous h-value, and make a list of the orbit. (For the images at the end of this section the maps were iterated from each initial point 1000 or more times, (5000 or 10000 for h-values $0.95,\ 0.99,$ and 1).)
3. Plot the orbits including transients.

   Note: the resulting behavior was checked by viewing the last 10 points of the orbit with the "*Part*" command in *Mathematica*. This somewhat verified whether the resulting behavior was a fixed point, a period two, or some other attracting object.

In Figure 7 the resulting behavior of one orbit within the basin is shown. This behavior can be seen to be either a periodic point, or a strange attractor. Recall that the exact behavior shown was produced from one selected point, and as such shows a specific orbit within the basin; additional points in the basin may have different beginning (transient) behavior, but all points within B_h for a single h value appear to have the same eventual behavior.

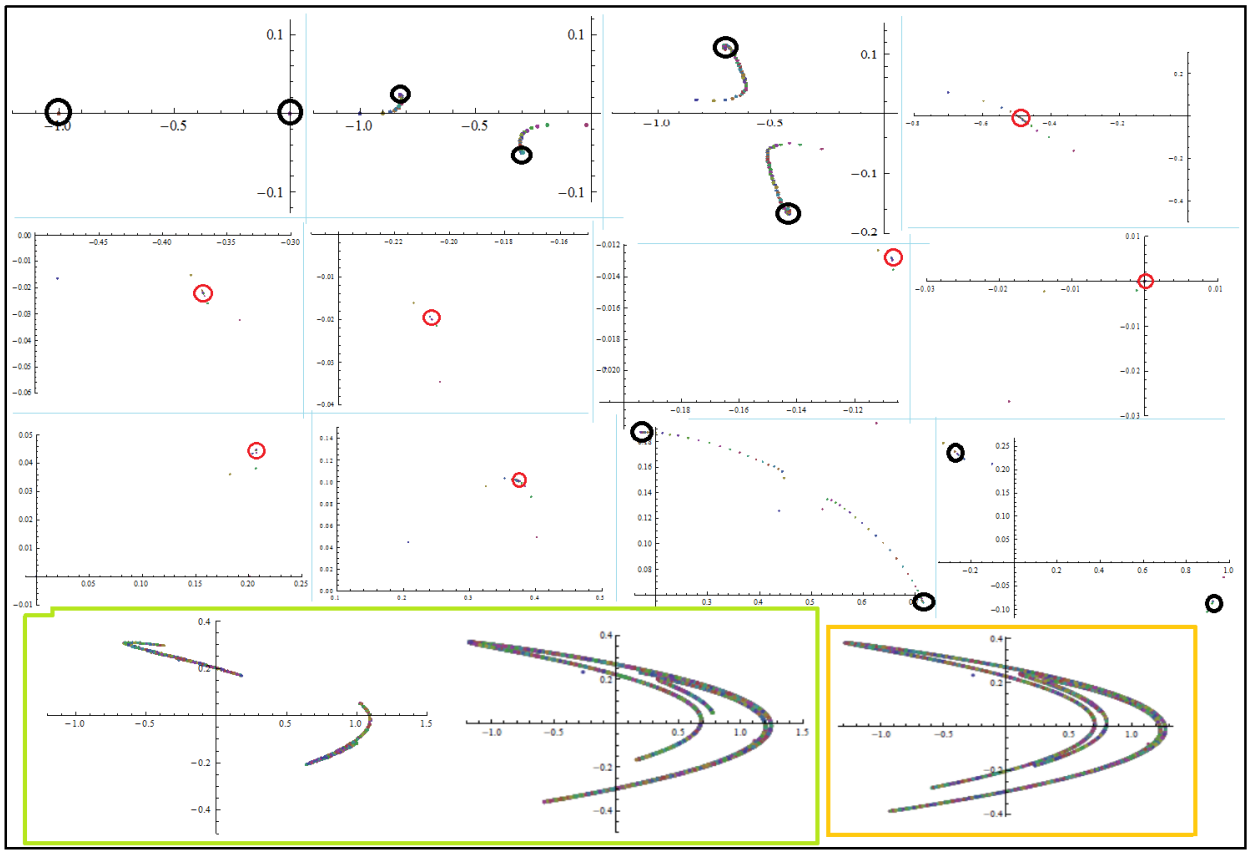

Figure 7

Orbit Behavior as h continues on $[0,1]$. The above figure displays images for $h = 0, 0.5, 0.1, 0.2, 0.3, 0.4, , 0.45, 0.5, 0.6, 0.7, 0.8, 0.9, 0.95, 0.99, 1$. Circled in red are fixed point attractors, circled in black are period two attractors, boxed in light green are attractors whose period is unknown if they even are periodic, and boxed in yellow is the strange attractor. All other points in each image are transient behavior.

4.2.Orbit Diagram

An orbit diagram depicts the attractors for a variety of different parameters (in our case for a variety of different h values). It only depicts attracting behavior; the algorithm does not show repelling or saddle periodic orbits. Conventionally graphed with the parameter on the horizontal axis and, for a two dimensional graph,

the x-coordinates on the vertical axis (ignoring the y-coordinate), the figures in the next section are as such. While graphing the attractors provides us a look at both coordinates in the plane (and transient behavior if wanted), producing an orbit diagram has the advantage of showcasing transitions of attractors as h changes.

4.2.1.Orbit Diagram Production

Orbit diagram production required steps 1 and 2 from the previous process for computation of attractors, mentioned in section 4.1. The only addition to the process was removing the transient behavior. From previous experimentation it appeared that up to $h = 0.9$ all the attractors were of period one or period two, so selecting only the last two values was necessary. For $h > 0.9$ selecting the last 500 values was appropriate. This final plot (Figure 8 on the following page) is the resulting orbit diagram.

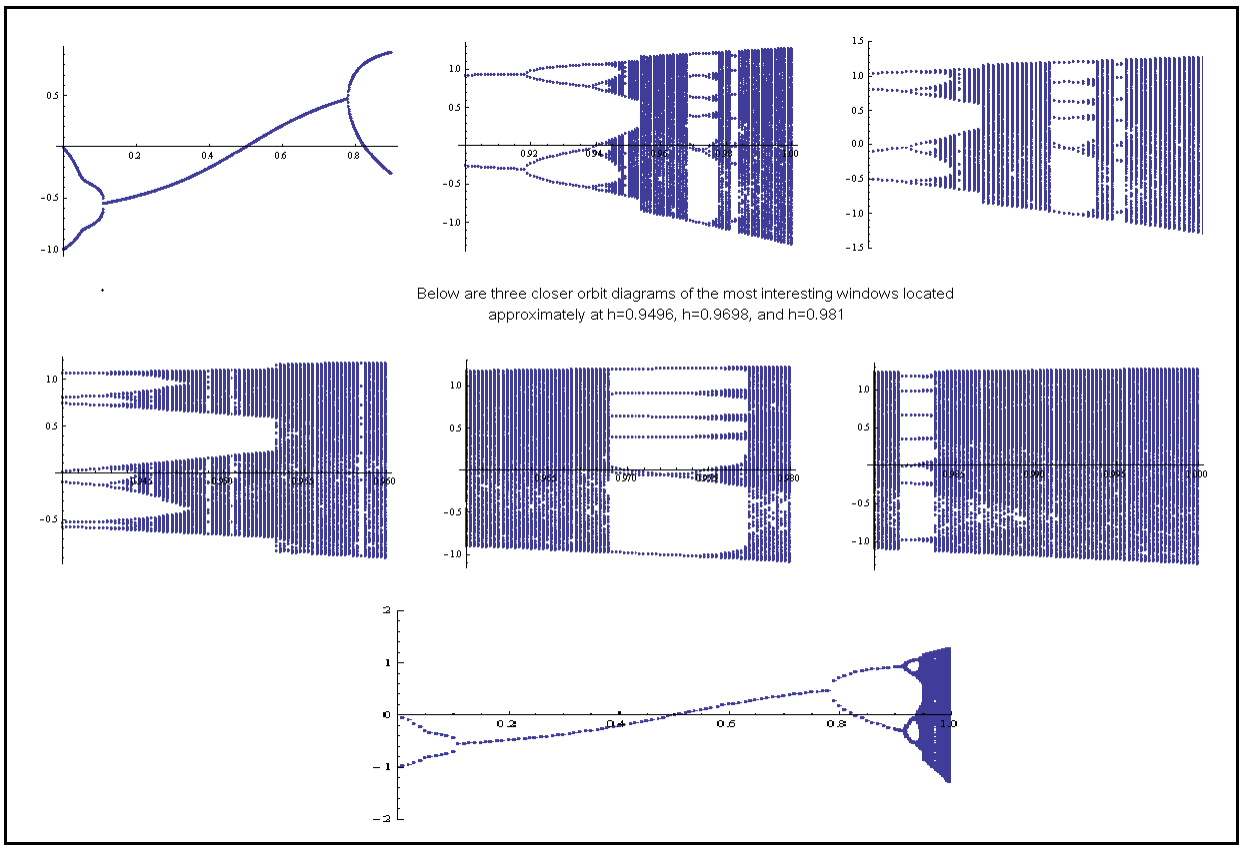

Figure 8

Multiple views of the homotopy's orbit diagram.

The bottom image is the complete view from $h = 0$ to $h = 1$, and the remaining images are enlargements of specific parameter ranges.

4.2.2.Orbit Diagram Comparison

As mentioned above, the behavior for h in $[0.9,1]$ is quite similar to the behavior witnessed for the logistic map, $\mu x(1-x)$, when $3 \leq \mu \leq 4$. Most like the logistic map, the homotopy's orbit diagram has a sequence of period-doublings (that is, has a period-doubling route to chaos) with "windows" of attracting period n's, where $n \epsilon \mathbb{Z}$. Different from the logistic map, though are quite a few things. First, the initial behavior of the graph, from $h = 0$ ($\mu = 0$ for the Logistic map)

until the first period-doubling, is of a different period. The logistic map begins with period ones, but for this homotopy the initial attractors are period twos leading into a period one. Second, the largest period n window is different. It appears, from numerical investigation, that this homotopy's largest window begins with a period six. While the logistic map's largest window begins with a period three. Third, and most interesting, the general shape of the period-doubling behavior is different on the top and bottom edges. The logistic map's outermost period-doubling curve is smooth as μ varies. This homotopy's outermost period-doubling curve has a jump near $h = 0.955$. What exactly causes this jump is unknown, but another one occurs near $h = 0.985$. Perhaps transient behavior is to blame for these events and whether this is or is not true, further analysis would need to be done in order to fully understand the entire orbit diagram. The graphical comparison can be seen on the next page in Figure 9.

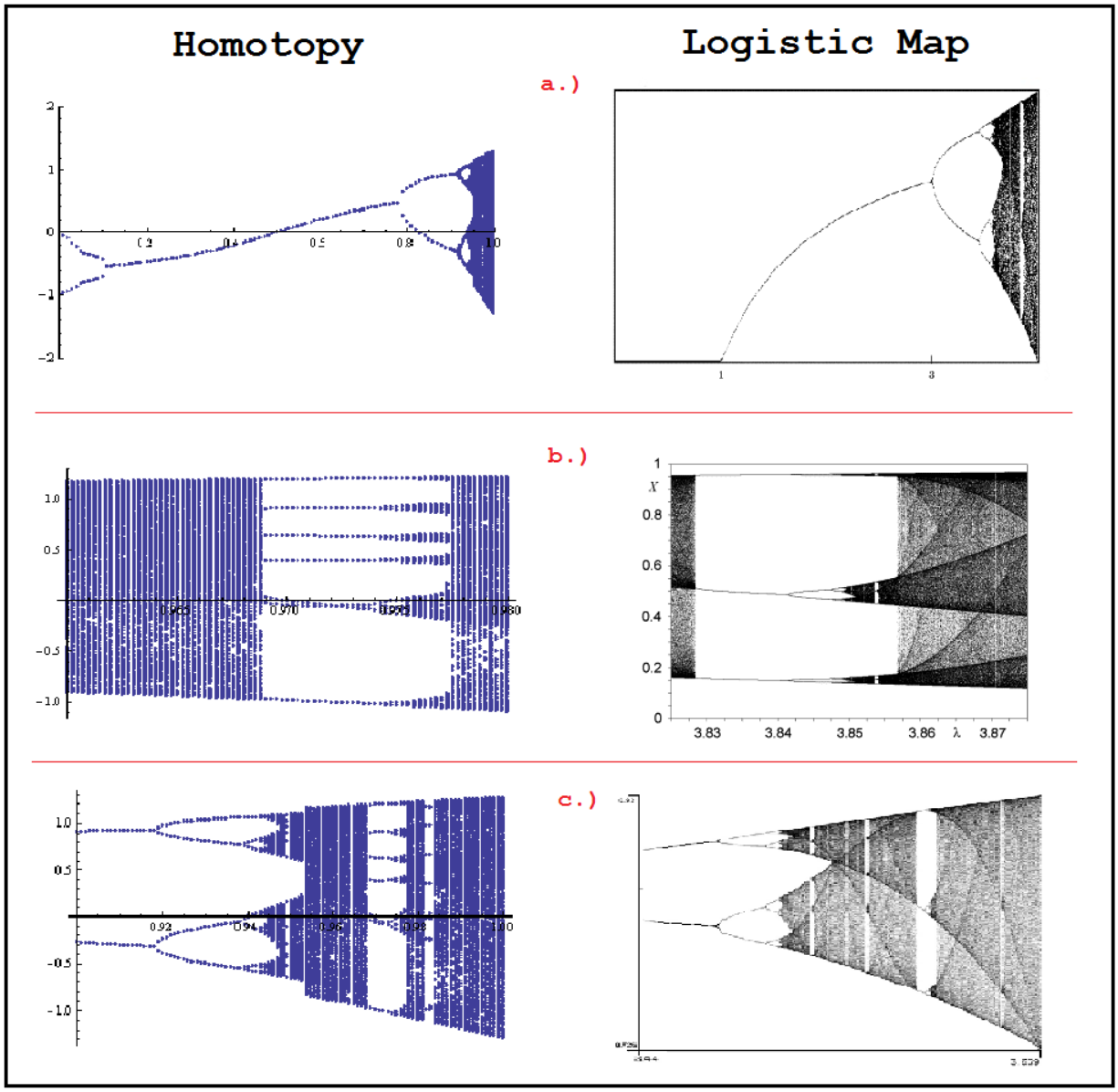

Figure 9 [6-8]

Graphical comparison of three aspects (see text) for the homotopy's and Logistic map's orbit diagrams. Displayed according to how they were addressed within section 4.2.2, based on zooms the reader should view then sequentially as a, c, b.

5.Periodic Points

Explicitly solving for periodic points in terms of h gave some challenging output when attempted using *Mathematica.* One issue was, without eliminating one of the variables first the output was hard to understand and almost impossible to use to calculate fixed points in terms of h. The other problem was when a single variable was eliminated, whether it was x or y, the solution to the one variable, one parameter equation was a large/irreducible solution. Hence it would not be a benefit to provide such an equation here. Providing *Mathematica* with fixed h-values though allowed the calculation of, period one (more frequently referred to as fixed points) and period two points. More numerically accurate than fixed and period two attractors obtained from iteration, *Mathematica* can also solve for fixed and period two points even if they are not attracting. These values helped offer more complete snap shots of the dynamics of the homotopy along with detailing interesting behavior associated with their movement and location in and/or around the basins of attraction.

5.1.Fixed Points

With a single-variable equation, fixed points are found by setting the function equal to its variable, say for example, $z^2 - 1 = z$. In words then, what this accomplishes is finding points that after a single iterate remain where they started. In this homotopy's case, it is necessary to set the function equal in both coordinates. Recall the above mentioned homotopy given in equation (3), its expanded form is as follows,

$$g_h(x, y) = (h(1 - 1.4x^2 + y) + (1 - h)(-1 + x^2 - y^2), 0.3hx + 2(1 - h)xy) \qquad (6)$$

In order to solve for fixed points, the system of equations we ask *Mathematica* to solve are:

$$h(1-1.4x^2+y)+(1-h)(-1+x^2-y^2)=x, \quad (7)$$
$$0.3hx+2(1-h)xy=y.$$

Our two end functions, the basilica map and the Hénon map, are solved with some work by hand. Known to be $\left\{\frac{1\pm\sqrt{5}}{2},0\right\}$, the basilica map's fixed points are found using the much simpler system of equations when $h=0$:

$$x^2-y^2-1=x, \quad (8)$$
$$2xy=y$$

Notice the bottom equation yields two solutions when all variables are brought to one side and factored.

$$2xy-y=y(2x-1)=0 \quad (9)$$

Only one solution provides real fixed points, when $y=0$ ($x=\frac{1}{2}$ leads to a complex value for y). Input this value for y into the first equation and solve for x:

$$x^2-0^2-1=x \Leftrightarrow x^2-x-1=0. \quad (10)$$

Solved just as quickly, though with less aesthetically pleasing and condensed solutions, the system of equations for the Hénon map is:

$$1-1.4x^2+y=x, \quad (11)$$
$$0.3x=y.$$

Plug the bottom equation, as an equation for y or solved for x, into the top and solve for the single variable:

$$1-1.4x^2+0.3x=x \leftrightarrow -1.4x^2-0.7x+1=0 \quad (12)$$
$$x=\frac{0.7\pm\sqrt{6.09}}{-2.8}$$

Plug solutions back into the bottom equation to get the full pairing.

$$0.3*\left(x=\frac{0.7\pm\sqrt{6.09}}{-2.8}\right)=y \quad (13)$$

Readily found, the fixed points for the Hénon map are approximately:

$$\{-1.1313544770895048, -0.3394063431268514\}, \{0.6313544770895047, 0.1894063431268514\}.$$

While fixed points for these two maps are fairly simple to find by hand, once the parameter h is chosen between 0 and 1 they become much more complicated to solve without software. With the help of *Mathematica* though, these systems of equations are quickly and accurately solved numerically for any fixed value of h, despite the fact there is not a nice explicit formula for each variable in terms of h. In order to show why this is the case included below are the polynomials used for solving for fixed points when one of the variables is removed:

In terms of x:

$$h^3x^2(-869.+960.x^2) + h^2x(-830.+2069.x + 1360.x^2 - 2320.x^3) + h(-200.+1200.x - 960.x^2 - 2160.x^3 + 1760.x^4) + 100.-300.x - 100.x^2 + 800.x^3 - 400.x^4 = 0$$

In terms of y:

$$hy(-150.+1560.y + 280.y^2 + 1200.y^3) + h^2(-9.+360.y - 1889.y^2 - 560.y^3 - 1200.y^4) + h^3(18.-231.y + 689.y^2 + 280.y^3 + 400.y^4) - y^2(500.+400.y^2) = 0$$

Notice that I have moved all terms to one side and that both of these equations are by no means simple polynomials of degree four. For this reason, simplifying these equations or their solutions merely made them messier and/or harder to understand.

5.1.1. Solutions with *Mathematica* for $h\epsilon(0,1)$

Utilizing the "Solve" command, solutions to equation (7) were computed for each parameter value, h. The real solutions were selected by hand and displayed using a list plot.

Note: It is worthwhile to mention here, the "ListPlot" command does not display any imaginary solutions, if one wanted to display them.

The figure below, Figure 10, displays fixed points for select h values along with the corresponding bounded and unbounded sets. Notice two things: how the fixed points stay in similar regions as h changes, but more interestingly how the outer fixed point moves from the right to left edge of K_h as h passes between 0.4 and 0.45.

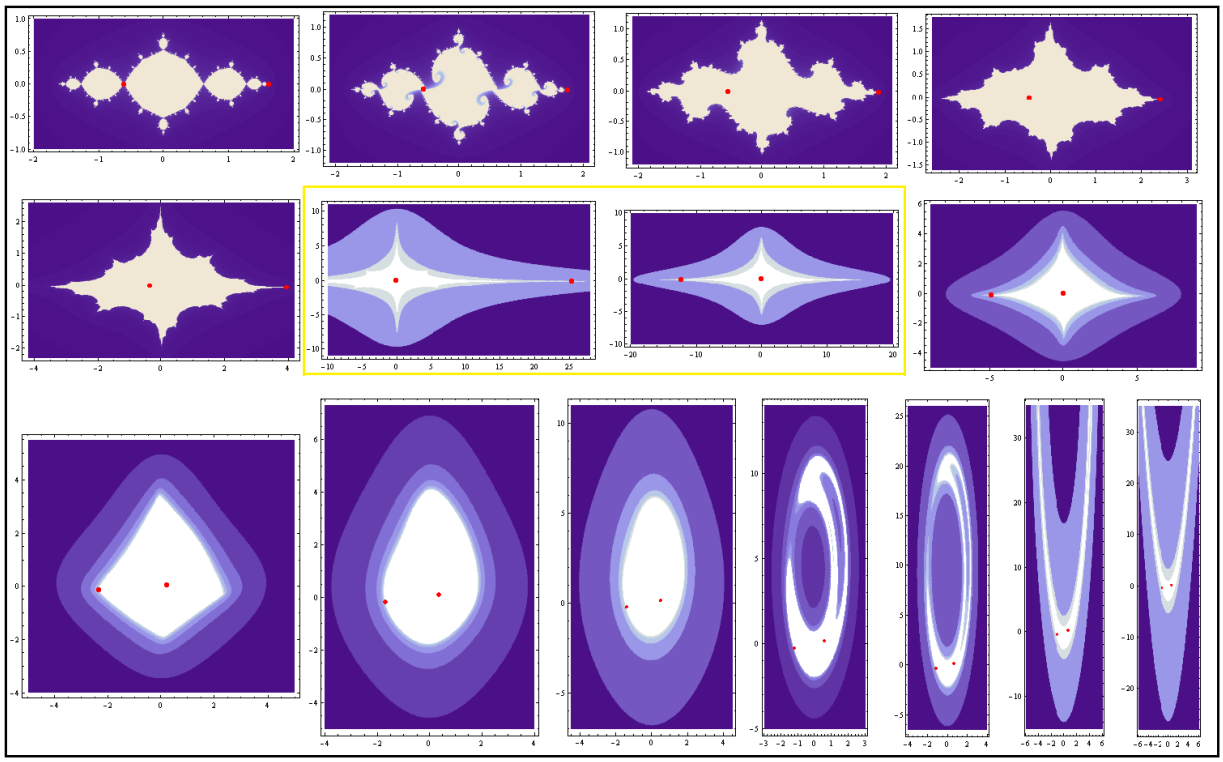

Figure 10

Fixed point locations within the basins of attraction for $h = 0, 0.056, 0.1, 0.2, 0.3, 0.4, 0.45, 0.5, 0.6, 0.7, 0.8, 0.9, 0.95, 0.99, 1$. Boxed in yellow, the location of a fixed point (within K_h) goes off to infinity as $h = \frac{5}{12}$ is approached from the left, and goes off to negative infinity as $h = \frac{5}{12}$ is approached from the right. This fixed point appears to be located on the boundary.

As we progress through the homotopy, images six and seven provide insight into what could be the first located bifurcation for this family of maps. Graphically, and with numerical support, the outermost fixed point goes off to infinity, and comes back in toward the basin from negative infinity on the opposite side (boxed in yellow above). Addressed in more depth in section 7, this bifurcation at infinity is not a standard bifurcation for continuous dynamical systems maps.

5.1.2. Identifying $h = \frac{5}{12}$ with *Mathematica*

As stated above, if it were possible to get solutions for periodic points, in terms of h, in an understandable and usable output then it would be possible to pinpoint the h value where the fixed point goes off to infinity. While this direct method was not possible; solving for just the h value by a similar method was possible, with the additional help of Dr. Harlan Stech. The method proceeded as follows:

> In a complicated output, *Mathematica* gave a solution to real fixed points (x, y) in terms of h but did so in terms of a "Root" expression. One of the solutions, when simplified for the single variable x, contained a cubic (in h) denominator which could be set equal to zero and solved for h. (Appendix B).

The resulting solutions provide three values, $h = 0$ (a double root) and, after rationalizing, $h = \frac{5}{12}$. Accordingly, $h = \frac{5}{12}$, is the other value (besides $h = 1$) for which Nien's Lemma does not guarantee a finite escape radius and for which a fixed point on the boundary goes off to infinity.

Recall in Section 3.1, images of mapped unit circles were produced under the quadratic terms of g_h and included the origin at both these values.

5.2. Period Two Points

Period twos, like fixed points, require solving a system of two equations. The system of equations, however, is taken from the second iterate of the homotopy rather than the original equation. That is, now we are asking *Mathematica* to solve,

$$g_h\big(g_h(x,y)\big) = (x,y), \tag{14}$$

a pair of 4^{th} degree polynomials of two variables that is much more complex even for this family of maps. What we find through this process are points that after two iterates map back to themselves. This process also finds fixed points again, but this time these values are ignored.

5.2.1. Solutions with *Mathematica*

With an almost identical procedure to that of finding fixed points, finding period twos required only the additional step of "nesting"; that is iterating the function twice before defining a list and displaying the points with a list plot. At the top of the next page Figure 11 illustrates period two points in relation to their basins of attraction.

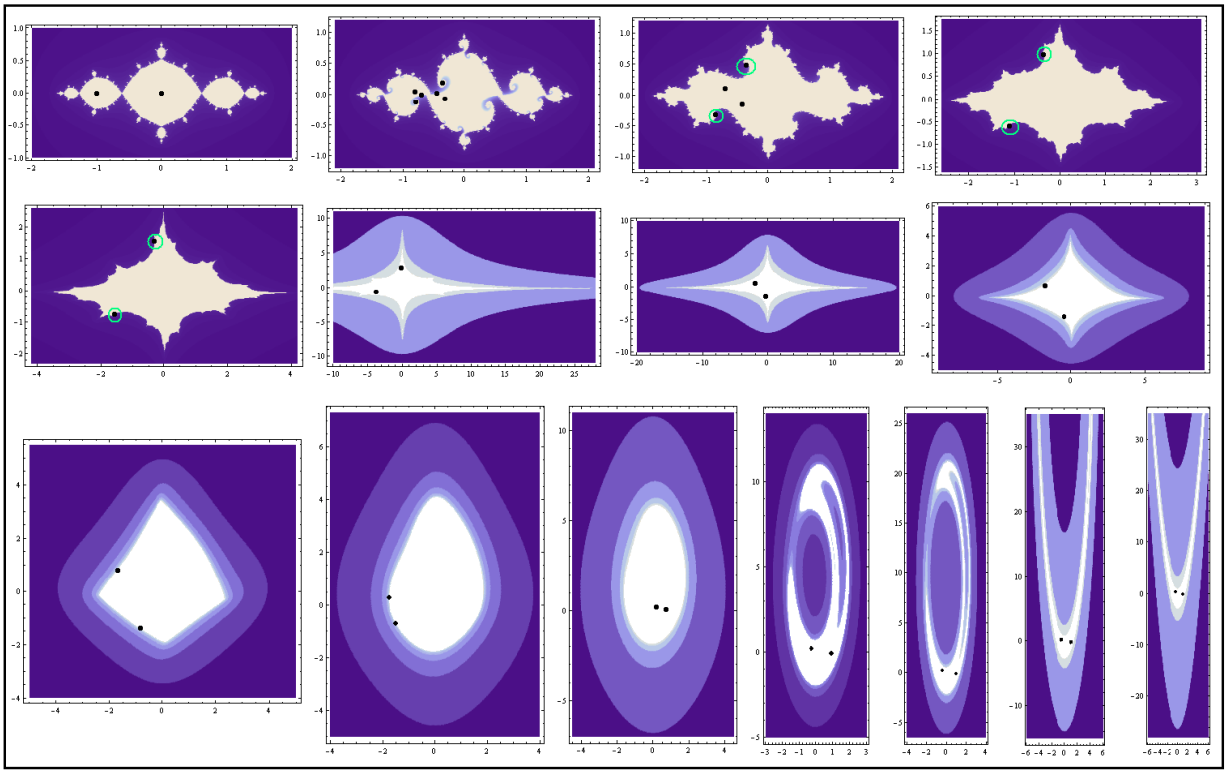

Figure 11

Period 2 points within their basins of attraction for $h = 0, 0.056, 0.1, 0.2, 0.3, 0.4, 0.45, 0.5, 0.6, 0.7, 0.8, 0.9, 0.95, 0.99, 1$. Certain period twos are circled simply because they are difficult to see.

5.2.2. Period Two Observations

While fixed points mostly moved horizontally and portrayed an interesting dynamic occurrence at infinity, period two points appear to move much more freely (at least initially) and provide telling details toward this homotopy. Keeping in mind, stabilities at this point had not been calculated toward any periodic points, influential graphical evidence still leads toward important conclusions. Images 1-2 could be indicating a saddle-node bifurcation, while images $2-5$ likely indicate that two period-doubling bifurcations occur as observed with the orbit diagram. Images 6 and 7 don't appear to be

indicating much about the critical value at $h = \frac{5}{12}$, however later when bifurcation diagrams are introduced (section 7.4), we will see that both period two points go off to infinity in what appears to be two different coordinate directions, as h approaches $\frac{5}{12}$ from either side. Images 10 and 11 indicate additional analysis is required to determine what is causing period two points to move from what appears to be the basin boundary into the interior of the basin (addressed in section 8). Along with determining whether or not some of these period twos are really on the basin boundary or whether it just appears that way.

6.Critical Sets

Critical sets, also called zero sets, are the values for which the Jacobian determinant equals zero,

$$|Jg_h| = \left\| \begin{bmatrix} \frac{-14}{5}hx + 2x(1-h) & \frac{3}{10}h + 2y(1-h) \\ h - 2y(1-h) & 2x(1-h) \end{bmatrix} \right\| = 0 \qquad (14)$$

$$-\frac{28}{5}x^2h(1-h) + 4x^2(1-h)^2 - \frac{3}{10}h^2 + \frac{3}{5}yh(1-h) - 2yh(1-h) + 4y^2(1-h)^2 = 0$$

and contains a map's critical orbits – the forward orbits of critical points. Critical sets help determine map dynamics. For example, for $z^2 + c$, if the critical point iterates to infinity, its filled Julia set is a Cantor set (an infinitely disconnected set). If not, its filled Julia set is a simply connected set. While no theorem like this applies to g_h, the critical sets are still important and do tell us where foldings in the map occur. Not surprisingly, the nature of the critical set changes at $h = \frac{5}{12}$ which coincides with the bifurcation at infinity. In a thesis titled *The Investigation of Saddle-Node Bifurcation with a Zero Eigenvalue – Includes Example of Non-Analycity* by Chia Hsing Nien (the same author as noted for the paper defining escape radii, K), chapter 5 addresses zero sets and their two-

dimensional conic images. If we are to assume the intermediate value theorem is correct from Section 3.1 – which it is – then from Nien's thesis we should have a transition of conic sections for the homotopy's zero sets. In Figure 12 select zero sets are shown, including this transition. Notice that as h approaches $\frac{5}{12}$ the zero set is an ellipse and then by $h = 0.45$ the zero set is a hyperbola with two branches. It turns out that there is a single h-value at which this transition occurs; the ellipse stretches and separates into two parallel lines. These parallel lines occur at exactly $h = \frac{5}{12}$, and are shown in the second figure, Figure 13.

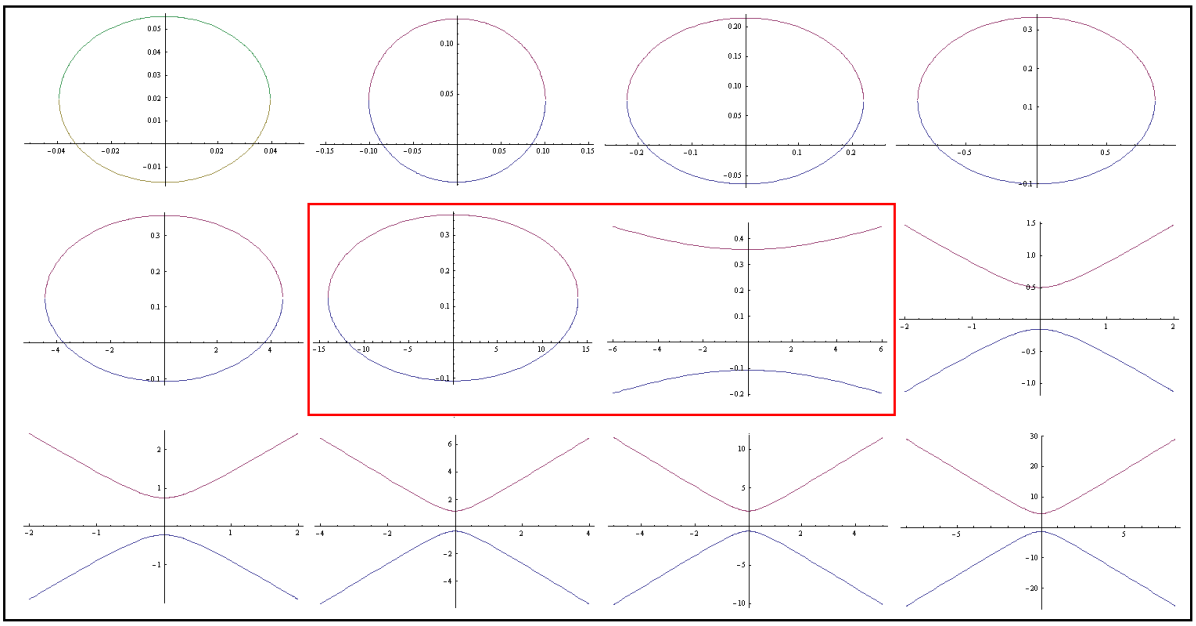

Figure 12

Zero set transitions as h continues on the interval $[0,1]$. Shown are the values

$$h = 0.1, 0.2, 0.3, 0.4, 0.41, 0.416, 0.417, 0.5, 0.6, 0.7, 0.8, 0.9$$

Not pictured here, the critical set for the basilica map is a single point at the origin, while the critical set for the Hénon map is empty.

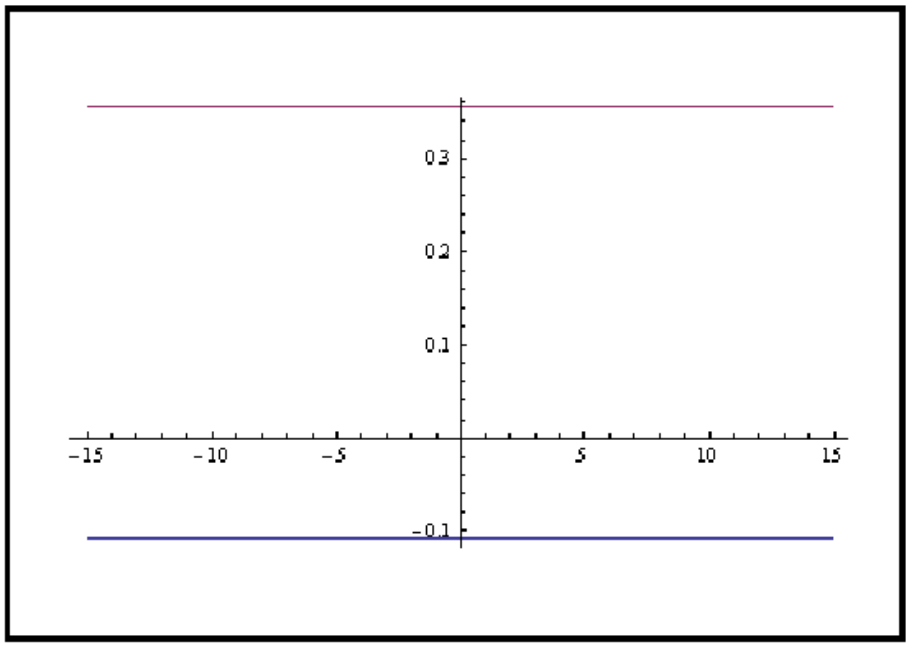

Figure 13

The zero set for $h = \frac{5}{12}$. Two parallel lines.

Note: This is an image of the parallel lines displayed. They were found by substituting $h = \frac{5}{12}$ into equation (14)and setting the determinant equal to zero:

$$\left|Jg_{\frac{5}{12}}\right| = \begin{bmatrix} 0 & \frac{1}{8}+\frac{7}{6}y \\ -\frac{7}{6}y+\frac{5}{12} & \frac{7}{6}x \end{bmatrix} = 0 \Leftrightarrow \frac{49}{36}y^2 - \frac{49}{144}y - \frac{5}{96} = 0$$

with solutions $y = -\frac{3}{28}, y = \frac{5}{14}$.

7.Bifurcation Classification

In order to classify bifurcations we must first have an understanding of each one. For any two-dimensional discrete dynamical system, the three simplest and most common ways to encounter a

bifurcation are based on the birth/death of periodic points and the change in their stabilities. They are:

1. A real eigenvalue of a periodic point crosses the unit circle at the point $(-1,0)$.
2. A birth and or death of a pair of orbits occurs, and an eigenvalue of 1 exists at the bifurcation value.
3. Two conjugate imaginary eigenvalues simultaneously cross out of or into the unit circle.

In order to know whether any certain periodic orbit's stability changes requires computing its eigenvalue(s) and checking to see whether any of them pass through the unit circle. Once the stabilities are found, analysis involves verifying them with their graphical counterparts. Stability definitions, based on eigenvalues, for the three types of periodic points, attracting, saddle, and repelling are presented in Appendix A. Stability analysis was completed after eigenvalue calculations were done in *Mathematica*. While the computations are not presented here, the stabilities are presented in the figures for each following section by the different types of lines. The key is as follows:

solid, thin red line: attracting fixed point branch
dashed red line: repelling fixed point branch
dot-dashed red line: saddle fixed point branch
solid, thin blue line: attracting period two branch
solid, thick blue line: spiral attracting period two branch
dashed blue line: repelling period two branch
tiny, dashed blue line: spiral repelling period two branch
dot-dashed blue line: saddle period two branch

7.1.The Period-Doubling Bifurcation

The first occurrence (1.) defines a period-doubling bifurcation provided that the stability of the periodic point branch changes as the period-doubling point is passed, and a period two orbit is born with the same stability as one of those periodic point branches. For this homotopy, numerical evidence show that four period doubling bifurcations occur from fixed points, one more period-doubling bifurcation occurs from a period two point, and a period-doubling sequence/period-doubling route to chaos, for multiple periods, occurs approximately on the interval, $0.92 \leq h \leq 0.984$. Below and on the following page are two figures. Figure 14 showcases the four period-doubling bifurcations from fixed points, and Figure 15 the period-doubling bifurcation from period two points along with the period-doubling route to chaos.

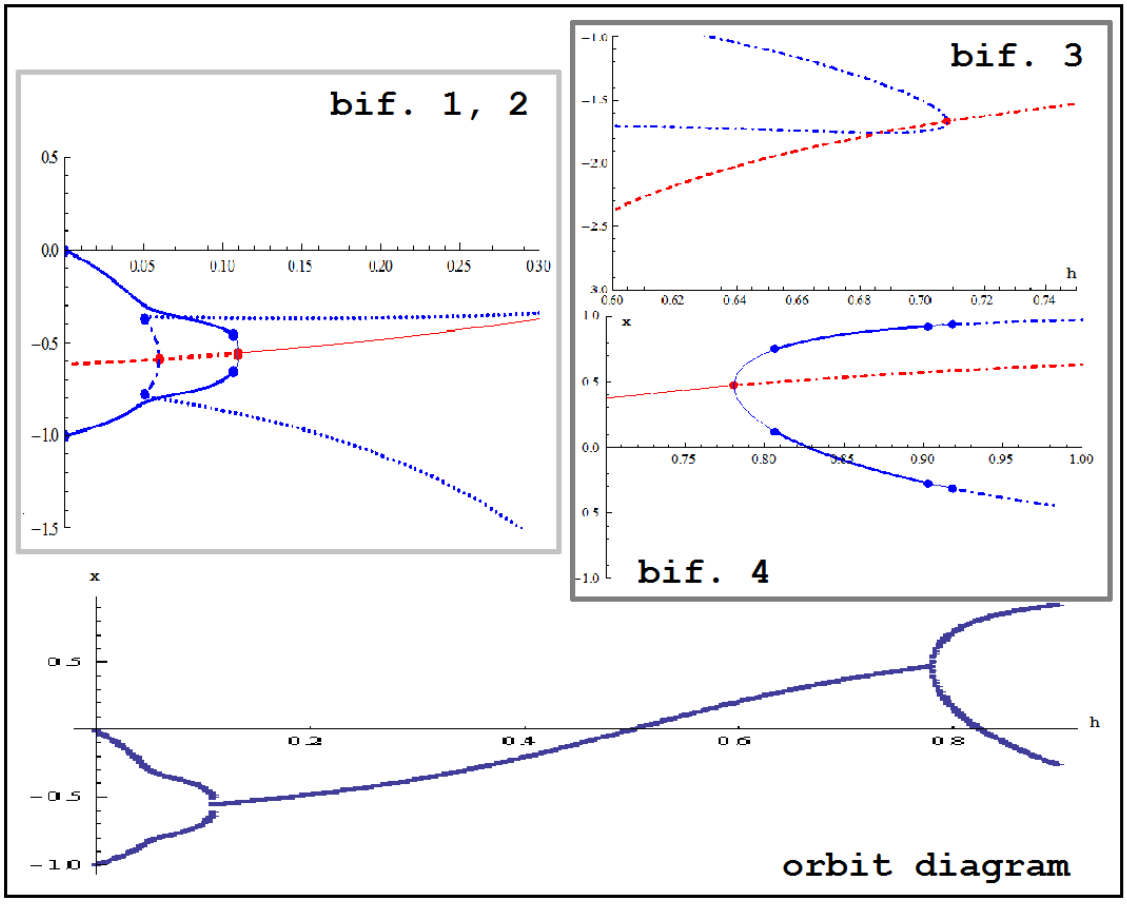

Figure 14 (caption on following page)

Fixed point bifurcations (Red Dots)

Bifurcation 1: Period-doubling at $h \cong 0.06$. Bifurcation 2: Period-doubling at $h \cong 0.11$. Bifurcation 3: Period-doubling at $h \cong 0.71$. Bifurcation 4: Period-doubling at $h \cong 0.78$. The orbit diagram and period two branches are provided to aid in showcasing the fixed point bifurcations. Period two bifurcations are addressed in the following figure.

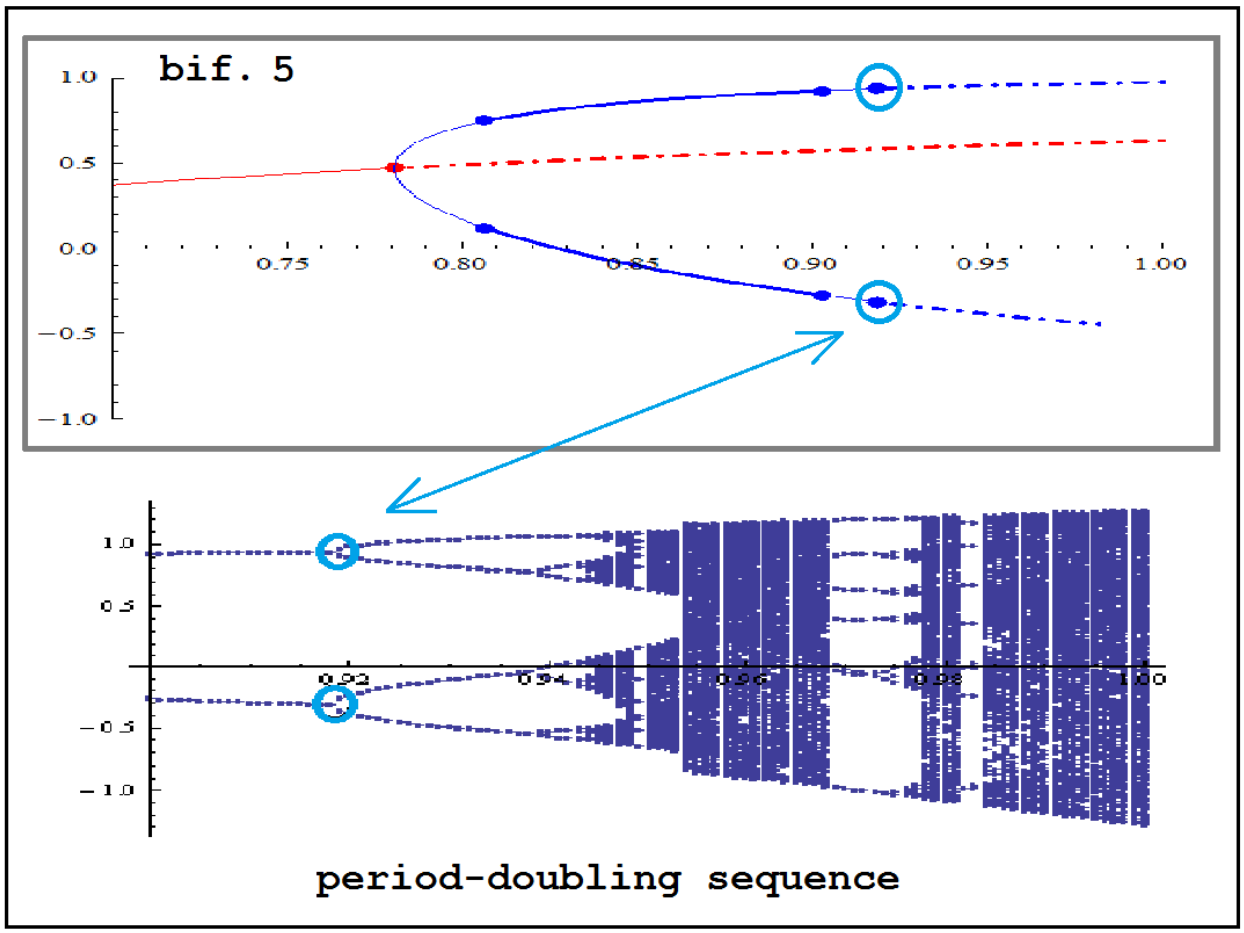

Figure 15

Period 2 (blue dot at $h \cong 0.92$) and period n bifurcations

Bifurcation 5: The above diagram shows the stabilities for the period two branch leading up to the period-doubling bifurcation. Seen only from the orbit diagram below, this occurrence is circled in light blue, and was not calculated from stabilities with *Mathematica* because period four calculations were not performed. The full period-doubling route to chaos is shown on the bottom and discussed in more depth in section 4.

7.2.The Saddle-Node Bifurcation

The second occurrence (2.) defines a saddle-node bifurcation. When we have the birth and or death of a pair of periodic orbits, we have this type of bifurcation. It is so named, because when this $0-1-2$ sequence occurs, one branch of the fixed point curve/line is a node (that is attracting or repelling) while the other is a saddle; hence the title, saddle-node. The image below (Figure 16) depicts this single occurrence for the period two branch at $h \cong 0.0505$.

Note: In order to see the birth of the pair of period two orbits it is necessary to look back at bif. 1, 2 in Figure 14. There, with the additional branches, it can be seen that for a very small region of h-values just passed this occurrence there are three period two orbits.

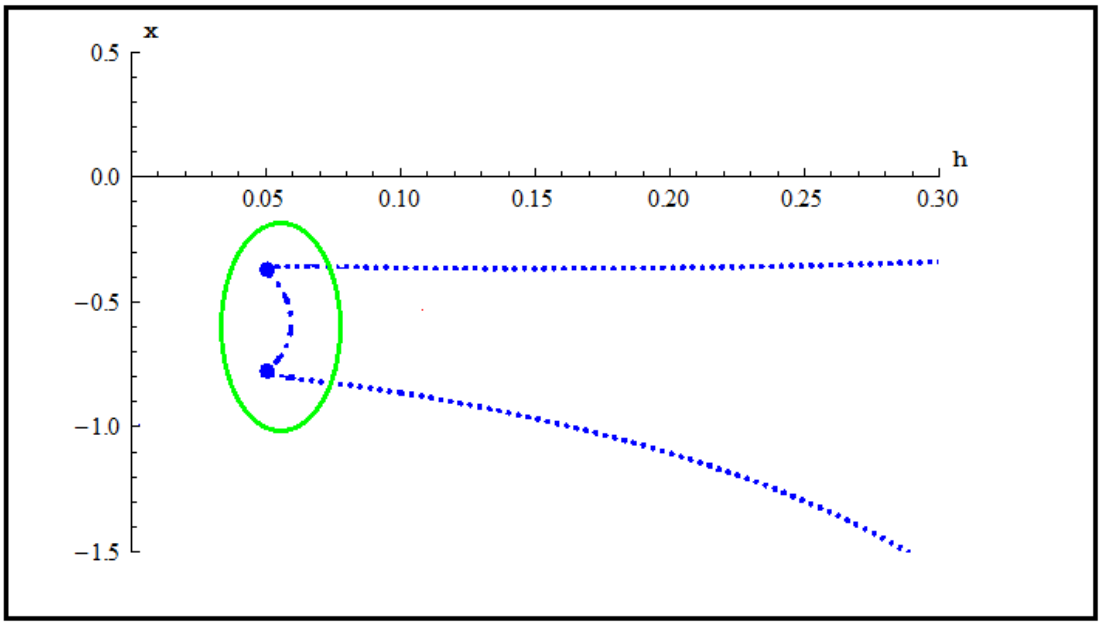

Figure 16

Isolated period 2 saddle-node bifurcation

7.3.Double Eigenvalues

The third occurrence (3.) for maps is a Hopf bifurcation. Defined when two complex-conjugate eigenvalues cross the unit circle. This homotopy does not appear to have a Hopf bifurcation, for fixed points or period two points, based on the analysis completed. Similar to the process for a Hopf bifurcation though, this family of maps does have eigevnalues that go from real to complex. In order for this occurrence to take place, we must have double eigenvalues. Since all of these double eigenvalues occurred on period two branches, we had two real eigenvalues become equal at a single h-value, and then separate as complex-conjugate eigenvalues. Analysis indicated we had five sets of double eigienvalues but none of them led to a Hopf bifurcation, because at no time did these complex-conjugate eigenvalues cross the unit circle; they remained in or out of the unit circle the entire time. Figure 17 shows where these double eigenvalues exist along the bifurcation diagram. Notice two sets of double eigenvalues occur just after a period-doubling bifurcation, and one set occurs just after the saddle-node bifurcation. The remaining two double eigenvalues occur when $h = 0$ and just before the period-doubling route to chaos.

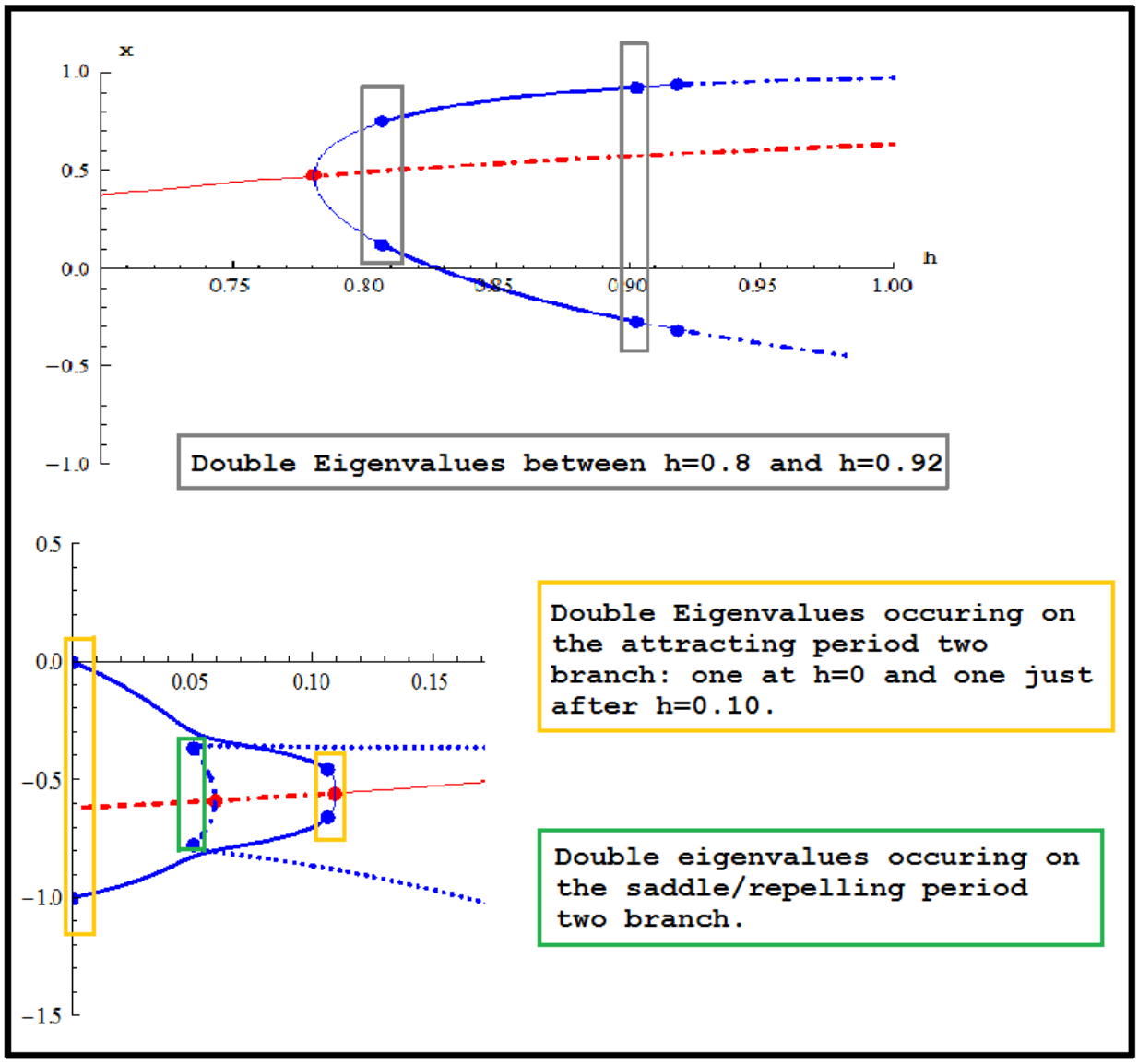

Figure 17

Double Eigenvalues (box colors corresponding to period two branches) Misleading in this figure, the double eigenvalues in the green box appear to be the same as the saddle-node bifurcation dots but are just too close to distinguish at this scale.

7.4 Bifurcation at Infinity

This map has an interesting event as h approaches $\frac{5}{12}$. Graphical investigation strongly indicates that there is a bifurcation occurring at infinity. Since no known research has been done for bifurcations similar to this with dynamical systems, it is hard to define or describe exactly what is happening. However, what we know about this occurrence is four-fold: the escape radius, a fixed point, the period two orbit, and the critical set all go off to infinity as we approach $h = \frac{5}{12}$ from either side. Notice in Figure 18 (on the following page), a fixed point appears to asymptote to infinity (in the x direction) from the left, and negative infinity from the right. Both points on the period two orbit go off to infinity, but it is a little misleading for both branches. The projected image of the bottom branch is actually asymptotic to negative infinity, and the upper branch goes off to negative infinity in the y-coordinate direction (which is not shown). See Figure 18.

Additionally, Dr. John Pastor noticed a connection between the parameter, a in the Hénon map and the value $h = \frac{5}{12}$. When $h = \frac{5}{12}$ is plugged into g_h he noticed that $h\left(= \frac{5}{12}\right) * 1.4 = \left(1 - \frac{5}{12}\right) = (1 - h)$. From this, a question arose: if we use a Hénon map with $b = 0.3$, but a is different, will we get another bifurcation at infinity where $a * h = (1 - h)$? A related observation began with noticing when $h = \frac{5}{12}$ is plugged into g_h the x^2 terms end up cancelling which makes the first argument of $g_{\frac{5}{12}}$ solely in terms of y. One can see then, that at $h = \frac{5}{12}$, $g_{\frac{5}{12}}$ maps horizontal lines to vertical lines:

$$g_{\frac{5}{12}} = \left(\frac{-1}{6}\right) + \left(\frac{5}{12}\right)y - \left(\frac{7}{12}\right)y^2, \left(\frac{1}{8}\right)x + \left(\frac{7}{6}\right)xy.$$

For any single y-value in the above equation, the first argument is some value and the second argument is linear in terms of x. Hence horizontal lines map to vertical lines.

7.5.Zero Eigenvalue

In some instances, the dynamics around a periodic point change but are not defined to be bifurcations. These events can sometimes lead us to future behavior/bifurcations, and other times simply tell us more about a map. For this homotopy a zero eigenvalue was encountered on a fixed point branch when $h \cong 0.356$. At this parameter value our map is not locally invertible. It is important to note that globally this is not the only parameter value for which the map is non-invertible. In fact all maps except g_1 are non-invertible. Also, for nearby parameter values the fixed point is stable. This last idea should make sense, because fixed points with small positive or negative eigenvalues are both stable. A bifurcation would not necessarily occur at a zero eigenvalue. Figure 18 on the next page singles out the bifurcation at infinity and the zero eigenvalue.

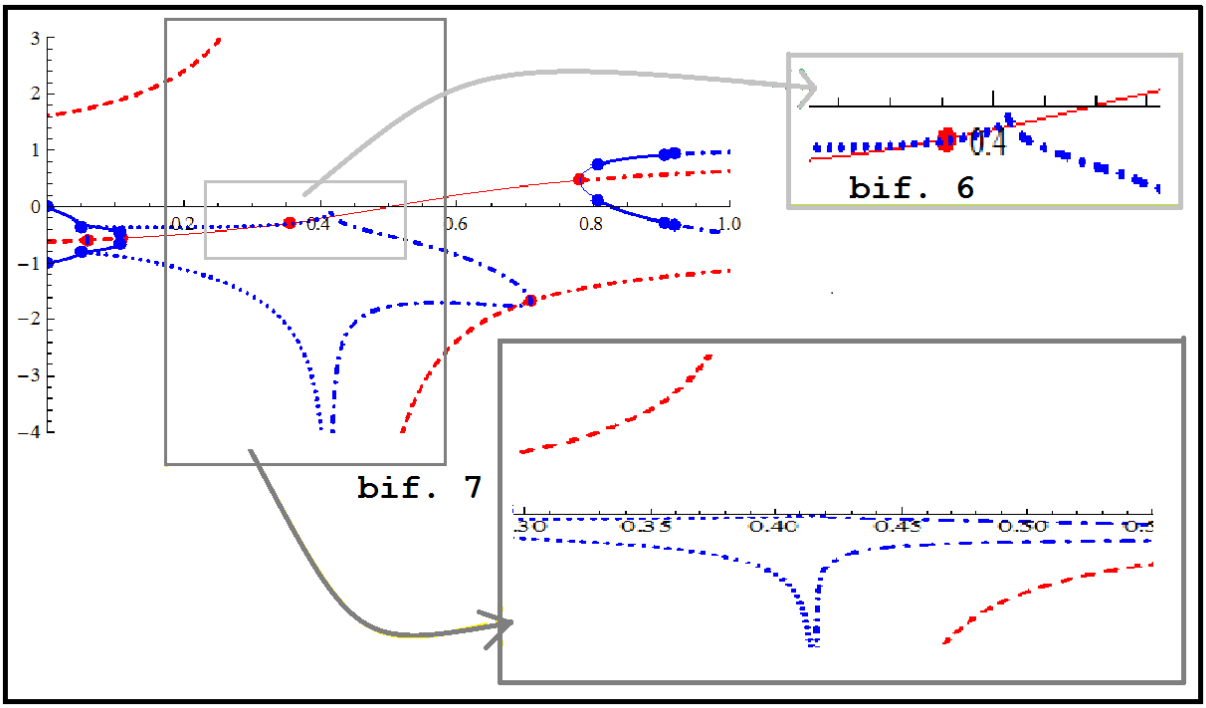

Figure 18

Zero Eigenvalue (red dot – bifurcation 6) and the Bifurcation at Infinity (asymptotic branches – bifurcation 7)

8. Summary

Figure 19 on page 43 is a summary of the dynamics as h progresses from 0 to 1. Ideally, a 3D figure connecting each object to the bifurcation diagram would be the best way to display and analyze the bifurcations. However, this is quite hard to render. So, the figure on the next page is a set of 2D graphs for select h values along with a bifurcation diagram. The bifurcation diagram at the top, has light grey lines inserted for the different h-values used to analyze the homotopy, and subsequent snap shots are the objects at those light grey lines.

All objects in the snap shots have already been addressed in earlier sections. Now compiled into a single figure, it is important to reiterate some key observations. First, when $h = 0.75$ there are no real period two points. As seen in the bifurcation diagram, there is a small region where none exist. This explains the movement witnessed in Section 5.2.1. Recall the period two points moved from what appeared to be J_h, into B_h. This did not take place as a "jump" but rather the real period two points disappeared onto one fixed point branch and then reappeared on another fixed point branch in B_h. Secondly, it is quite surprising that when $h = 0.9$, the attractor is a period two and yet changing h by just $.05$ toward the Hénon map, the attractor is of a period unknown, or possibly non-periodic. Following points within different K_h may lead to a better understanding of this event. Thirdly, in a more general sense, the dynamics as a whole leading up to and after the critical value $h = \frac{5}{12}$ are quite different. Simply looking at K_h, leading up to $h = \frac{5}{12}$ the bounded orbits somewhat resemble the basilica map and then stretch out. After $h = \frac{5}{12}$, K_h condenses back in and then elongates vertically, resembling nothing like the fractal structure J_h began with. Yet finally, and most important, the occurrence at $h = \frac{5}{12}$ was neither expected nor familiar. To have a bounded set of orbits go off to infinity in the middle of the family

of maps gave some interesting dynamics. For example, one fixed point and the period two orbit have gone off to infinity, the basin for the remaining attracting fixed point extends to infinity also, and its zero set is two parallel lines. Aside from its numerical and graphical properties though, this bifurcation at infinity is motivating. To come across something that really has no research or information regarding it is exciting. Could there be another map with similar dynamics near/at infinity? What would the differences be, and what could these differences indicate? Could a change of coordinates tell us more about what is happening at infinity? Answers to these could help better understand this bifurcation. For now though, this map and the information provided will have to be a starting point for possible dynamics and bifurcations for discrete dynamical systems.

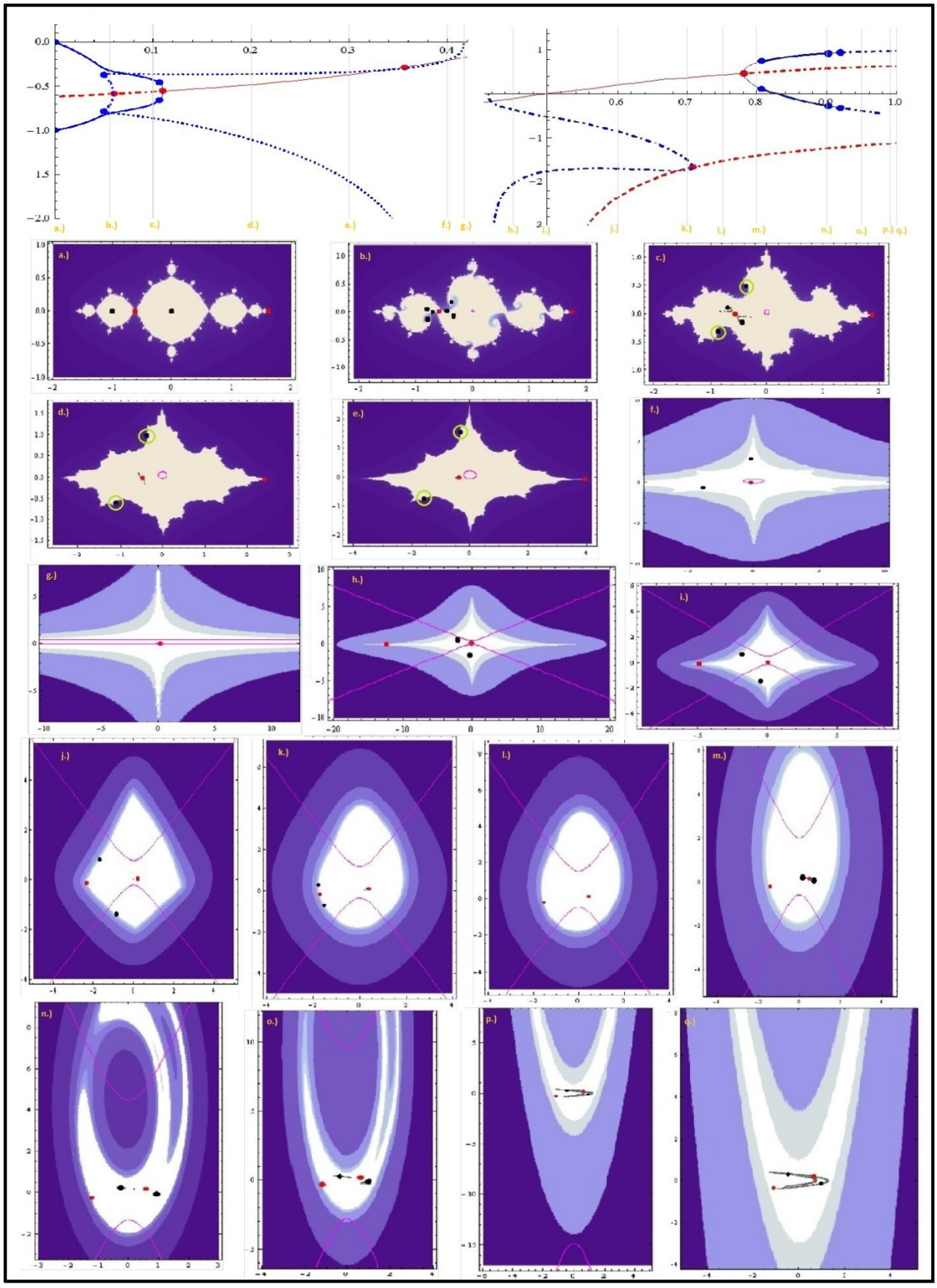
a.)
b.)
c.)
d.)
e.)
f.)
g.)
h.)
i.)
j.)
k.)
l.)
m.)
n.)
o.)
p.)
q.)

Figure 19 (Previous Page) [10]

Bifurcation Diagram and Snap Shots of Homotopy for

$h = 0, 0.056, 0.1, 0.2, 0.3, 0.4, \frac{5}{12}, 0.45, 0.5, 0.6, 0.7, 0.75, 0.8, 0.9, 0.95, 0.99, 1$.

Appendix

A. Stability Definitions

In general, eigenvalues are found by setting up the function's corresponding matrix and solving it, depending upon the matrix's size, by the simplest procedure necessary. For two-dimensional maps, this requires the computation of a Jacobian matrix, comprised of partial derivatives for each parameter. The common form for a Jacobian matrix is:

$$\begin{pmatrix} \frac{\partial F_1}{\partial x_1} & \cdots & \frac{\partial F_1}{\partial x_n} \\ \vdots & \ddots & \vdots \\ \frac{\partial F_m}{\partial x_1} & \cdots & \frac{\partial F_m}{\partial x_n} \end{pmatrix}.$$

For this homotopy in particular though, the Jacobian matrix form used was:

$$\begin{pmatrix} \frac{\partial g_1}{\partial x} & \frac{\partial g_2}{\partial x} \\ \frac{\partial g_1}{\partial y} & \frac{\partial g_2}{\partial y} \end{pmatrix}.$$

From here, eigenvalues are then found by a common procedure for 2x2 matrices, calculate:

$$A - \lambda I$$

(where A is the Jacobian matrix and I is the identity matrix)

and then solve its determinant:

$$(a - \lambda)(d - \lambda) - bc\,.$$

Since each determinant is a polynomial of degree two, there will be two eigenvalues for each periodic point. The definitions given in *An Introduction to Chaotic Dynamical Systems Second Edition* by Robert

Devaney, categorize the stability of a periodic point by determining the absolute value of each real solution. That is, we check λ as follows:

- If λ satisfies $|\lambda| < 1$ for both eigenvalues, then the fixed point is attracting (a sink).
- If λ has a value such that one eigenvalue satisfies $|\lambda| < 1$ and one eigenvalue satisfies $|\lambda| > 1$, then the fixed point is a saddle.
- If both solutions for λ satisfy $|\lambda| > 1$, then the fixed point is repelling (a source).

Note: For period two points, the Jacobian matrix was set up from the second iterate equation, as described in Section 5, and for certain h values had complex eigenvalues. For these, categorizing was the same but in the first and last case, attracting becomes spiral attracting (spiral sink) and repelling becomes spiral repelling (spiral source).

B. *Mathematica* for $h = \frac{5}{12}$

```
f[{x_, y_}] := {x^2 - y^2 + c1, 2 * x * y + c2}

c1 = -1;
c2 = 0;

d1 = 14 / 10;

d2 = 3 / 10;

H[{x_, y_}] := {1 - d1 * x^2 + y, d2 * x};
g[h_, x_, y_] := h * H[{x, y}] + (1 - h) * f[{x, y}];

S1 = Solve[g[h, x, y] == {x, y}, {x, y}, Reals]

X = x /. Simplify[%]

MatrixForm[X]

MatrixForm[N[X]]
```

```
ConditionalExpression[- 10. Root[-9 h^2+18 h^3+(-150 h+360 h^2-231 h^3) #1+(-500+1560 h-1889 h^2+689 h^3)
  / (-3. h+20. (-1.+h) Root[-9 h^2+18 h^3+(-150 h+360 h^2-231 h^3) #1+(-500+1560 h-1889 h^2+
ConditionalExpression[- 10. Root[-9 h^2+18 h^3+(-150 h+360 h^2-231 h^3) #1+(-500+1560 h-1889 h^2+689 h^3)
  / (-3. h+20. (-1.+h) Root[-9 h^2+18 h^3+(-150 h+360 h^2-231 h^3) #1+(-500+1560 h-1889 h^2+
ConditionalExpression[- 10. Root[-9 h^2+18 h^3+(-150 h+360 h^2-231 h^3) #1+(-500+1560 h
  / (-3. h+20. (-1.+h) Root[-9 h^2+18 h^3+(-150 h+360 h^2-231 h^3) #1+(-500
ConditionalExpression[- 10. Root[-9 h^2+18 h^3+(-150 h+360 h^2-231 h^3) #1+(-500+1560 h
  / (-3. h+20. (-1.+h) Root[-9 h^2+18 h^3+(-150 h+360 h^2-231 h^3) #1+(-500

#1^2+(280 h-560 h^2+280 h^3) #1^3+(-400+1200 h-1200 h^2+400 h^3) #1^4 &,1]
689 h^3) #1^2+(280 h-560 h^2+280 h^3) #1^3+(-400+1200 h-1200 h^2+400 h^3) #1^4 &,1]) , 1. < h < 1.49119 || h > 1.49119 || h < 1.]
#1^2+(280 h-560 h^2+280 h^3) #1^3+(-400+1200 h-1200 h^2+400 h^3) #1^4 &,2]
689 h^3) #1^2+(280 h-560 h^2+280 h^3) #1^3+(-400+1200 h-1200 h^2+400 h^3) #1^4 &,2]) , 1. < h < 1.49119 || h > 1.49119 || h < 1.]
-1889 h^2+689 h^3) #1^2+(280 h-560 h^2+280 h^3) #1^3+(-400+1200 h-1200 h^2+400 h^3) #1^4 &,3]
+1560 h-1889 h^2+689 h^3) #1^2+(280 h-560 h^2+280 h^3) #1^3+(-400+1200 h-1200 h^2+400 h^3) #1^4 &,3]) , 1. < h < 1.49119]
-1889 h^2+689 h^3) #1^2+(280 h-560 h^2+280 h^3) #1^3+(-400+1200 h-1200 h^2+400 h^3) #1^4 &,4]
+1560 h-1889 h^2+689 h^3) #1^2+(280 h-560 h^2+280 h^3) #1^3+(-400+1200 h-1200 h^2+400 h^3) #1^4 &,4]) , 1. < h < 1.49119]
```

```
Plot[X, {h, 0, 1}]

Solve[
 -3.` h +
   20.` (-1.` + h)
    Root[-9 h^2 + 18 h^3 + (-150 h + 360 h^2 - 231 h^3) #1 + (-500 + 1560 h - 1889 h^2 + 689 h^3) #1^2 +
      (280 h - 560 h^2 + 280 h^3) #1^3 + (-400 + 1200 h - 1200 h^2 + 400 h^3) #1^4 &, 1] == 0, h]

{{h → 0.}, {h → 0.}, {h → 0.416667}}

Rationalize[0.4166666666666667`]

 5
12
```

C. Further Research

This project allows for numerous areas of continued and further research:

1. This homotopy can be continued for more accuracy with the addition of:
    - period 3 and higher periodic points
    - smaller h-value increments or all functions in terms of h so that a complete depiction of the transition can be given
    - Validating periodic points on the boundary are on the boundary (or contradicting this)
    - 3D representations
    - Applying a non-"straight line" homotopy
2. Additional homotopies can be further studied in order to:
    - Classify/group homotopies for chaotic dynamical systems
    - Gather more information regarding bifurcations at infinity
    - Study the differences for homotopies from chaotic dynamical maps to non-chaotic dynamical maps.

References

1. Hirsch, Morris W., Stephen Smale, and Robert L. Devaney. *Differential Equations, Dynamical Systems, & An Introduction to Chaos.* Second ed. San Diego, CA: Academic, 2004. Print.

2. Devaney, Robert L. *An Introduction to Chaotic Dynamical Systems*. Second ed. Redwood City, CA: Addison-Wesley, 1989. Print.

3. *Juliasetcreator*. Google Project Hosting, n.d. Web. May-June 2011. <http://code.google.com/p/juliasetcreator/source/browse/>.

4. Nien, Chia-Hsing. "The Dynamics of Planar Quadratic Maps with Nonempty Bounded Critical Set." *International Journal of Bifurcation and Chaos* 8.1 (1998): 95-105. Print.

5. McClure, Mark. Lecture. Julia Set Lab. University of North Carolina at Asheville, Asheville.*Generating Julia Sets with Mathematica*. Mark McClure. Web. May-June 2011. <http://facstaff.unca.edu/mcmcclur/class/FractalILS/JuliaSetLab.pdf>.

6. *The Orbit Diagram for the Logistic Map*. N.d. Photograph. *Reverse Bifurcations in a Unimodal Queueing Model*. By James A. Walsh. ScienceDirect, 14 June 2006. Web. July 2012. <http://www.google.com/imgres?q=logistic+map+period+doubling&hl=en&biw=1366&bih=643&tbm=isch&tbnid=-5_3mrLFzVJykM:&imgrefurl=http://www.sciencedirect.com/science/article/pii/S0097849306000884&docid=3HYEBEqliNcbAM&imgurl=http://ars.sciencedirect.com/content/image/1-s2.0-S0097849306000884-gr1.gif&w=561&h=673&ei=TWzqT-HbBuyA2QWRmIDHAQ&zoom=1&iact=hc&vpx=179&vpy=67&dur=396&hovh=246&hovw=205&tx=125&ty=82&sig=115447833609500556919&page=4&tbnh=143&tbnw=119&start=71&ndsp=27&ved=1t:429,r:6,s:71,i:319>.

7. *Period-3 Window in the Logistic Map's Bifurcation Diagram.* N.d. Photograph.*Cryptanalysis of a Discrete Chaotic Cryptosystem Using External Key*. By G. Alvarez, F. Montoya, M. Romera, and G. Pastor. ScienceDirect, 29 Oct. 2003. Web. July 2012. <http://www.google.com/imgres?q=logistic+map+period+3+window&hl=en&biw=1366&bih=643&tbm=isch&tbnid=hn-FIZb2xglSoM:&imgrefurl=http://www.sciencedirect.com/science/article/pii/S0375960103015603&docid=QvUAF2MjQpJiUM&imgurl=http://ars.sciencedirect.com/content/image/1-s2.0-S0375960103015603-gr001.gif&w=346&h=253&ei=VmvqT_7oOOnE2wW2gfWmAQ&zoom=1&iact=hc&vpx=903&vpy=152&dur=888&hovh=192&hovw=263&tx=116&ty=108&sig=115447833609500556919&page=1&tbnh=137&tbnw=189&start=0&ndsp=19&ved=1t:429,r:4,s:0,i:84>.

8. *The Bifurcation Diagram of {Qc(x)}.* N.d. Photograph. *Characteristic Polynomials Traversing the Bifurcation Diagram of the Logistic Map*. By Dean Whelton. 05 Dec. 2005. Web. July 2012. <http://welbog.homeip.net/~inferno/math/pmath370/>.

9. Nien, Chia-Hsing. *The Investigation of Saddle Node Bifurcation with a Zero Eigenvalue - Includes Examples of Non-analyticity*. Thesis. University of Minnesota, 1997. Ann Arbor: UMI, 1997. Print.

10. F., Dave. "How Can I Create a Vertical Line Using the Plot Command?" Web log comment.*MathGroup Archive 2009*. Wolfram, 25 Oct. 2009. Web. July 2012. <http://forums.wolfram.com/mathgroup/archive/2009/Oct/msg00656.html>.

11. *Wikipedia*. Wikimedia Foundation, 16 July 2012. Web. June-July 2012. <http://en.wikipedia.org/>.

Software

Wolfram Mathematica 7. Vers. 7.0. Champaign: Wolfram Research, 2008. Computer software

To Be Continued…. Vers. 5.3.7. Duluth: Bruce Peckham, (1986-present). Computer software <http://www.d.umn.edu/~bpeckham/tbc_home.html>